

Jovian decametric radio emission: An overview of the planetary radio astronomical observations

S K Bose^{1,2}, S Sarkar¹ & A B Bhattacharyya¹

¹Department of Physics, University of Kalyani, Kalyani 741 235, WB, India

²Department of Physics, Kalyani Govt. Engineering College, Kalyani 741 235, WB, India

Received 25 August 2005; accepted 5 November 2007

The paper presents an overview of the Jovian decametric (DAM) radio emission up to the recent years. Evidences for periodic modulation of Jupiter's DAM radio emission are considered first. Information of *Io* (Jupiter's Galilean satellite) and non-*Io* related source location and their characteristic features of emission, e.g., polarization, shape of the beam, L-bursts, S-bursts, N-bursts, modulation lane etc. are discussed. Broadband electrostatic noise and field aligned current sources at Earth and Jupiter have been taken into account. The scope and direction for further investigations is also pointed out.

Keywords: Jovian planet, Decametric radio emission, L-bursts, S-bursts, N-bursts

PACS No: 96.30.Kf, 95.85.Bh

1 Introduction

Jovian radio emission was first serendipitously discovered at decametric (DAM) wavelengths by Burke and Franklin¹ at the frequency of 22.2 MHz. Since that time, Jupiter has proven to have a wealth of complex radio emission (Fig. 1) mechanisms among the zoo of solar system radio emissions. It is seen from Fig. 1 that Jupiter (boldface) is often as intense as solar type III radio bursts. Of these complex radio emission spectra, the DAM region of the spectra, which is of present interest, has been sorted out. Jovian DAM has been systematically monitored for half a century, since its discovery from different terrestrial stations of varying latitude and longitude². As the emission can be detected from ground based stations from the upper cut-off frequency 39.5 MHz (Fig. 2) down to terrestrial ionospheric cut-off frequency, around 5-10 MHz and peak of the intensity of emission at around 8 MHz, it has been felt to investigate the emission from stations above ionosphere of the Earth, e.g. Earth orbiters³ Radio Astronomy Explorer (RAE1 and RAE2) and recently with radio and plasma wave instrument (WAVES) on the Wind space craft⁴. Then successively Jupiter's magnetosphere has been viewed *in-situ* by the spacecrafts⁵⁻¹⁷ — Pioneer 10 and 11, Voyager 1 and 2, Galileo, Ulysses and Cassini and all have noticed that as the terrestrial observations, there are different sources emitting radio emissions from the magnetosphere of Jupiter in the DAM range. The occurrence probabilities of detecting the emission

depend strongly on the coordinates of the Jovian central meridian longitude (CML), phase of Jupiter's Galilean satellite *Io* (*Io*-DAM) and related with same CML, but, independent of *Io*-phase (non-*Io* DAM), and the Jovicentric declination (D_E) of the Earth, respectively.

Klecker *et al.*¹⁸ analysing Galileo spacecraft data showed that Callisto, and to a lesser extent, Ganymede, influence Jovian radio emission as well. Ever since Bigg¹⁹ identified the dramatic correlation between the orbital positions of the Galilean moon *Io* and the observed occurrence probability and intensity of Jupiter's sporadic decametric (DAM) radio emission, investigators have tried to understand the mechanism underlying this effect^{20,21}. The emissions occur in episodes called "storms", which can last from a few minutes to several hours. Three types of bursts can be received during a storm. The L-bursts (L for long) that vary slowly in intensity with time and the S-bursts (S for short) or milli-second bursts which are sporadic spikes and N-bursts (N for Narrow band). Sometimes all the three types of bursts are present simultaneously. The emission is believed to beam into a thin hollow cone²². Radio-spectral observations^{21,23} by Voyager 1 and 2 spacecrafts (Fig. 3), Wind/WAVES data and Nancay-data²⁴ showed that the emission has a distinctive arc-like appearance on a frequency-time spectrogram²⁵. These types of phenomenon have also been confirmed from the data of radio and plasma wave science (RPWS) instrument¹⁷ on Cassini during the approach to

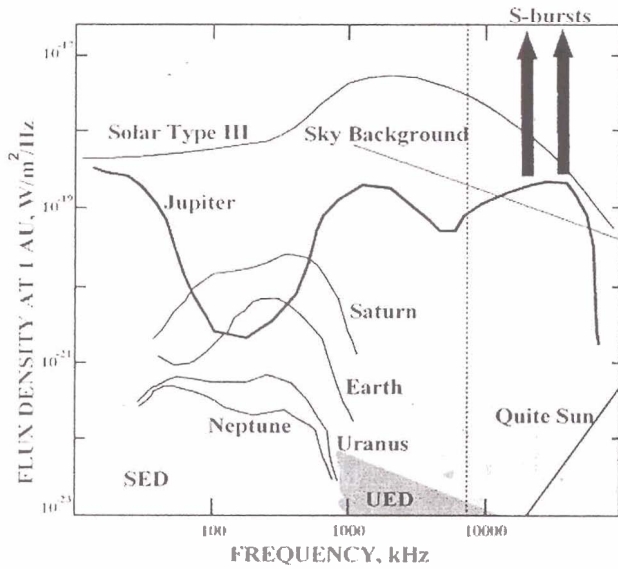


Fig. 1 — Average spectra (flux density against frequency) in the decameter-to-kilometer range, normalized to a distance of 1 AU (except for the sky background – Kraus, 1986) of the auroral radio emissions of the five “Radio-planets” [Peak levels are ~ one order of magnitude above these averages. Status of Jovian radio emission (boldface) is among the zoo of solar system radio emissions. Jovian S-burst fluxes can reach $10^{-16} \text{ Wm}^{-2} \text{ Hz}^{-1}$. Grey-shaded regions labeled “SED” and “UED” (Saturn/Uranus Electrostatic Discharges) – range of intensities of these planetary lightning-associated radio emissions. (Adapted from Zarka, 1992).]

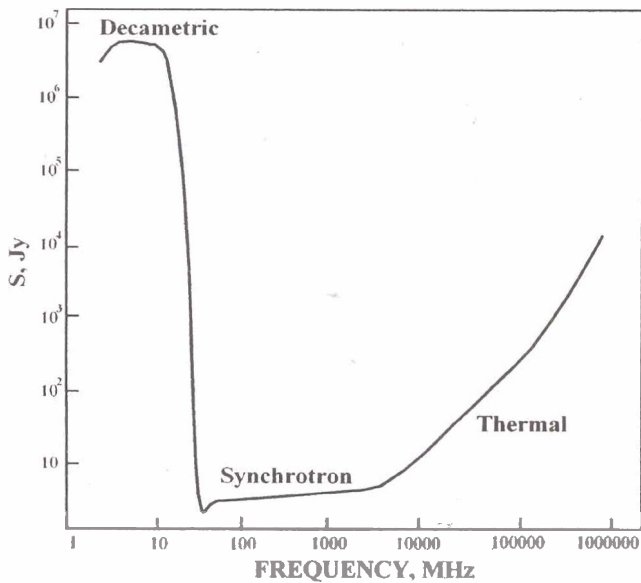


Fig. 2 — Jupiter’s decametric radiation at frequencies < 40 MHz [After that the range shows synchrotron and thermal range of spectrum. Courtesy Imke de Pater (UC Berkeley)]

Jupiter. These arc-like features are believed to be generated at the local electron-cyclotron frequency via the cyclotron maser mechanism²⁶⁻²⁸, which produces radiation nearly perpendicular to the local

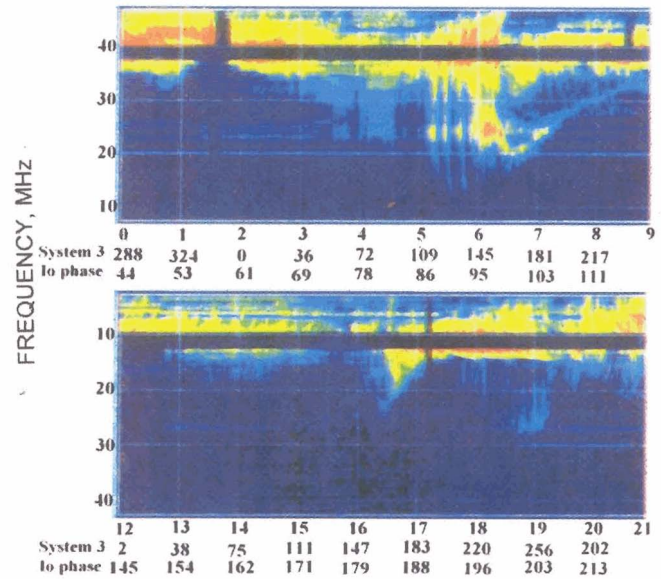


Fig. 3 — *Io*-B dynamic spectrum [(Vertical axis – frequency; Horizontal axis – top: time in hrs UT, middle: system III longitude, bottom: *Io*-phase) based on the total power, recorded by Voyager Spacecraft on 16 July, 1979: <http://www.astro.ufl.edu/voyager/gif/v2h197.gif>]

magnetic field²⁹. Usually, two types of arcs can be identified, *Io*-controlled and non-*Io* controlled. The *Io*-controlled arcs are produced by a system of Alfvén Waves excited by *Io*³⁰⁻³³. Non-*Io* controlled emissions are independent of *Io*’s position and are highly variable.

Evidence already exists that the solar wind plays a role in controlling the non-*Io* radiations³⁴⁻⁴⁸ and from the simultaneous observations using the Cassini and Galileo spacecraft data Gurnett *et al.*⁴⁹ showed that radio emission in the Hectometric (HOM) range and DAM range of non-*Io* origin as well as extreme ultraviolet auroral emissions from Jupiter are triggered by interplanetary shocks propagating outward from the Sun. Analysing the data from Galileo, Menietti *et al.*⁵⁰ showed that non-*Io* DAM emission from Jupiter has local time effect. Morioka *et al.*⁵¹ analyzed 551 non-*Io* related DAM events during the study period (17 years from 1 Oct. 1974 to 31 Dec. 1990) and 27 of the largest DAM events (4.9%) with the power index values of more than 400 were selected as huge DAM storms. They confirmed through the typical case studies that large solar wind disturbances trigger the huge DAM events which should have resulted from the Jovian magnetospheric disturbance. The result implies that even the large Jovian magnetospheric disturbance appears in a major singular event without sequential activities. From this

argument, it would be supposed that the Jovian magnetosphere unloads the stored magnetospheric energy in a burst and has no geomagnetic storm-like disturbance.

In this paper, periodic modulation of Jovian DAM and *Io* related source locations, and their characteristic features have been considered, e.g., polarization, L-bursts, S-bursts, N-bursts, modulation lane and the shape of the beam in a greater detail. Emphasis is also laid on the non-*Io* related features. Dynamics of the field-aligned current sources, both on the Earth and the Jupiter has also been taken into consideration. Finally, scope for further investigation has been discussed in detail.

2 Periodic modulation of radio emission

The role of Jupiter and *Io* in their mutual interaction and the nature of their coupling were first elaborated in greater detail by the two Voyager flybys in 1979. Subsequent exploration of this system by ground-based and Earth-Satellite-borne observatories and by the Galileo orbiter mission in 1995 and latest *in-situ* observation by Cassini in 2000 has improved the understanding of the highly complex electro-dynamical interaction between *Io* and Jupiter manifolds. Gurnett and Goertz⁵² proposed that the electro-dynamic interaction between *Io* and Jupiter's magnetic field could launch an Alfvén wave along the field lines near *Io*. This would undergo multiple reflections at Jupiter's northern and southern polar ionosphere, causing a standing wave current system extending down stream and moving with *Io* (Fig. 4). They estimated that at least nine reflections would be generated and each of these is associated with a discrete decametric radio source. The calculated longitudinal spacing between successive reflections in *Io*'s rest frame would be 5.8° with an error of factor of 2. Precise calculations by Bagenal⁵³ using an offset tilted dipole magnetic field model and a plasma density model of the *Io* plasma torus derived from Voyager 1 measurements⁵⁴ revealed that the actual spacing would vary with longitude in the plasma torus due to changing in the local Alfvén wave speed and the orientation and intensity of the magnetic field. It was concluded that the average longitudinal spacing between successive reflections would be 10° . If both north and south directed Alfvén waves are taken into consideration, this spacing would be expected to produce an average temporal separation between adjacent spectral arcs of 35 min.

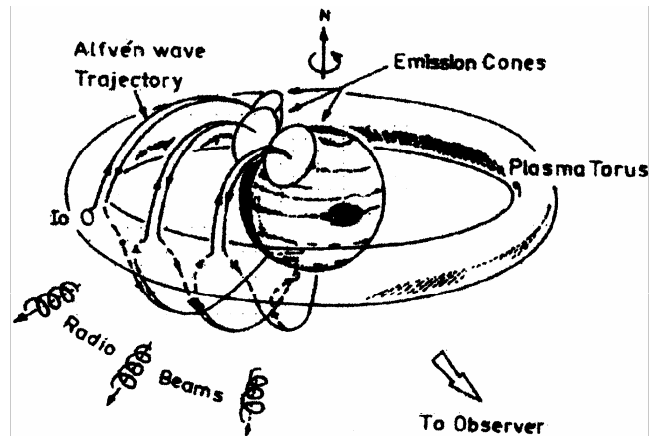


Fig. 4 — Standing Alfvén wave current system downstream of *Io* and the associated hollow emission cones corresponding to *Io*-related source [Carr *et al.*, *Physics of the Jovian Magnetosphere*. Ed. A J Dessler, 1983, p.226.]

Smith and Wright⁵⁵ gave an alternative explanation of the Alfvén wave interaction between *Io* and the Jovian magnetic field. They argued that Wentzel-Kramers-Brillouin (WKB) approximation assumed by Gurnett and Goertz⁵² in their model was inappropriate, owing to the enormous increase in Alfvén wave speed near the torus boundary, which might lead to significant wave reflection⁵⁶ with only 30% of the wave energy arriving at the polar ionosphere. This limits the number of ionospheric reflections of the Alfvén downstream of *Io* and hence reduces the extent of the standing wave current system. In Smith and Wright's model⁵⁵ the magnetic field disturbance created by *Io*'s orbital motion through the Jovian magnetic field manifested itself as an oscillation of the global magnetic field downstream of *Io*. They showed that magnetic field disturbance could be quantised using a series of Eigen mode solutions to the Sturm-Liouville equations. Wright and Smith⁵⁷ developed a model for the evolution of *Io*'s Alfvén waves considering a realistic magnetic field and torus density distribution by calculating the normal modes of the field lines disturbed by *Io* and synthesizing the waves near *Io* from a complex sum over the eigenmodes. In terms of the Jovian CML of a stationary observer, the authors expected large-scale structure ($> 60^\circ$), small-scale structure ($< 6^\circ$), and intermediate periods too in the wave pattern produced downstream from the satellite. These periodic structures are close to the observed intervals in decametric (DAM) radio emissions, such as the duration of a DAM storm, bunching of arcs within such a storm, and individual arc separation.

Staelin *et al.*⁵⁸ using the Voyager dynamic spectral data measured an average time interval of 3-4 min between adjacent arcs, equivalent to approximately 0.5° of *Io* phase. Also the time interval between arcs was randomly distributed in time, conforming to a Poisson distribution of intervals. In order to account for this discrepancy, they argued that many reflections of the Alfvén wave must occur, extending completely around Jupiter many times and thus overlapping to produce smaller apparent arc spacing. Using a completely different approach, Bagenal and Leblanc⁵⁹ reformatted the Voyager dynamic spectral data into epochs at fixed central meridian longitude and varying *Io* phase to simulate what an observer at fixed Jovian longitude would observe as the standing wave current system and the associated emission cones are carried past by *Io*'s orbital motion. They noted periodic gaps in the 'reconstructed' spectrographs, which were attributed by them to the spaces between Alfvén wave reflections. To simulate correctly these gaps using a model of the Alfvén wave wake down stream of *Io*, they increased the accepted values of plasma density^{60,61} in the *Io* plasma torus by 36%. Bagenal and Leblanc's assumption may be corroborated by the observation made by Galileo Space craft's data. Galileo measured ion plasma densities that were about 50% greater than those observed by Voyager at the same distance^{62,63}. Again to explain the observed multiplicity of closely spaced arcs, each Alfvén wave reflection had to be associated with multiple arcs instead of a single arc, a feature not yet explained properly with current theories of DAM generation²⁵⁻²⁸.

Wilkinson⁶⁴ suggested that Alfvén wave reflections might be identified not with individual arcs but with certain long duration arc structures as noted in the Voyager dynamic spectral data by Boischoit *et al.*²³ These arc structures contain substructures made up of individual arc-shaped segments, which are observed inside a single arc-shaped envelope and are readily distinguished from normal arcs. They have been referred to as "Principal arcs"⁶⁵ or *Io* caused emission (ICE) structure⁶⁶. These ICE structure should be generated when magnetic field lines corotating with Jupiter were stimulated for producing radio emission as they passed by *Io*. Wilkinson⁶⁴ developed an empirical principal arc-model in which the emission cone angle varied with frequency in a manner as suggested earlier by Goldstein and Thieman⁶⁷. This model was used to simulate principle arcs seen in the Voyager dynamic spectral data⁶⁵. Further, although

the principle arcs identified by Riddle⁶⁶ were all located either in the *Io*-A or *Io*-C region, the principal arc model could also account for some of the intense *Io*-related spectral arcs associated with the *Io*-B source. In searching evidence of the multiple principle arcs from sources within the extended standing wave current system down stream of *Io* in the Voyager dynamical spectral data Wilkinson⁶⁴ was able to identify a small number of examples in both the *Io*-A and *Io*-B regions. He deduced angular spacing within the range 9.8° - 14.8° between successive Alfvén wave reflections in the *Io* plasma torus, which is in satisfactory agreement with the 10° spacing predicted by Bagenal⁵³. A serious limitation of this study was that magnitude of the emission cone angle and its evolution with time, both of which had a vital role on the accuracy of the result, were essentially unknown at the time.

Wilkinson⁶⁸ hypothesized that if multiple radio beams were generated by the Alfvén wave interaction between *Io* and Jupiter and these beams were swept sequentially past the observer by *Io*'s orbital motion, the probability of receiving the emission would vary periodically with time, showing maxima when each beam was directed towards the observer (Fig. 4). Multiple (vertex early) arcs might be observed⁶⁸ in the frequency-time spectrogram taken close to the planet. But if observations were taken at a single frequency using a ground-based telescope, the effects of ionospheric and interplanetary scintillation would break up the arc emission. Such a periodicity should be observable as a periodic variation in L-burst activity with time. Bagenal and Leblanc⁵⁹ in their study, found periodicity in the Voyager dynamic spectral data and from this they deduced a longitudinal spacing of 13° between successive Alfvén wave reflections in the *Io* plasma torus. In the theoretical model of Wright and Smith⁵⁷ a low frequency modulation of the dominant quasi-periodic magnetic field perturbation is predicted when *Io* is in the upper portion of the torus as it is during *Io*-B storms. Moreover, this low-frequency modulation could account for the apparent splitting of the *Io*-B source into two components, *Io*-B1 and *Io*-B2, as described by Leblanc⁶⁹. Thus it seems plausible that two major periodicities could be present simultaneously in the data. Interestingly, in the *Io*-B data of Bagenal and Leblanc⁵⁹ there were examples of intense multiple principal arc emission where the angular spacing between the arcs expressed in *Io*-phase was much less than 13° . Prangé *et al.*⁶³ detected

for the first time far-ultraviolet (FUV H2 bands) spots at the *Io*-flux tube (IFT) foot prints (Fig. 5) with the Hubble Space Telescope Faint Object Camera (HST/FOC). Their observation supported the multiple reflecting Alfvén wave model^{25,30,70}. Similarly, infrared (IR) observations⁷¹ (Fig. 6) from NASA's infrared telescope showed single intense IR spot located 15°-

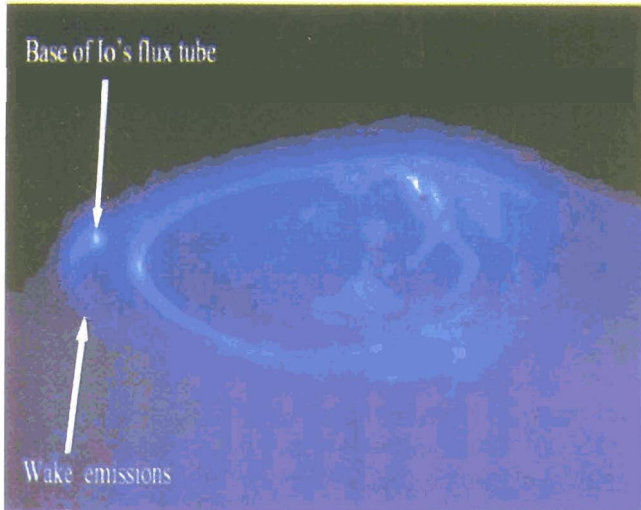


Fig. 5 — Shows an ultraviolet picture of the aurora and the *Io* footprint auroral emissions taken by the Space Telescope Imaging Spectrograph (STIS) aboard the Hubble Space Telescope (HST) in 1998 [Adapted from Thesis of Vincent Dols, 2001, p.12.]

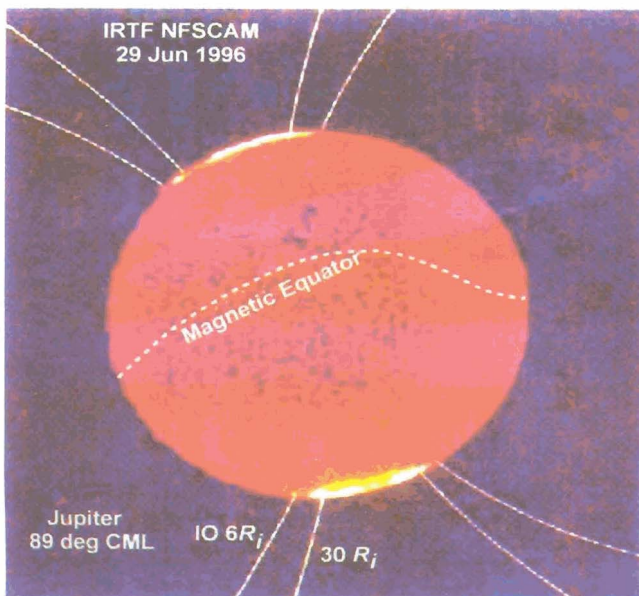


Fig. 6 — Infrared image at 3.4 μm of Jovian aurora and the *Io* footprint emissions Jupiter taken with NASA's Infrared Telescope Facility (IRTF) at Mauna Kea in 1995, Hawaii, using the NSFCAM facility imager [Connerney and Satoh, 2000]

20° of longitude down stream of the *Io*-foot print. Comparing these results with Jovian DAM radio bursts Prangé *et al.*⁶³ and Zarka *et al.*⁷² had built a scenario of the electron precipitations along the IFT for interpreting Jovian S-bursts and energy budget for the said phenomena.

An alternative explanation for the observed periodicity and the imaging data was that all of the DAM radio emission is generated in a single source at or near the *Io* footprint and is beamed into multiple directions⁶⁸. This explanation also considers the significant longitudinal extent of the Jovian DAM radio sources without requiring multiple Alfvén wave reflections down stream of *Io*. Further, both the diffraction theory of Lecacheux *et al.*⁷³ and the lasing theory of Calvert⁷⁴ provided a potential mechanism for explaining how multiple radio beams can be generated by a single source. However, polarization measurements during long-lasting *Io*-B storms⁷⁵⁻⁷⁷ revealed that the measured emission cone angle does not vary over a period of several hours, a feature in accordance with the multiple emission beam models. According to these models it would be expected that the emission cone angle should vary with time since *Io*'s position with respect to the observer changes.

3 *Io*- and non-*Io* related source locations and their characteristic features

3.1 Source locations and polarization

The long-term Earth-based observations² showed three prominent peaks of emission probability corresponding to longitude of Jupiter facing the Earth (central meridian longitude or CML). These sources are usually labelled sources A (around 240° CML), B (around 150° CML), and C (around 330° CML). The exact location and magnitude of the peaks of probability varies slowly depending on frequency in the 15 MHz – 40 MHz frequency range. Below 15 MHz there is a sudden shift in the picture to two peaks of probability, one around 180° CML the other one around 330° CML. Hence to investigate the phenomena, observations from above the ionosphere have been continuing by Earth orbiters³ and spacecrafts⁴⁻¹⁷. Spacecraft observations of this transition region are limited. The Voyager Planetary Radio Astronomy (PRA)^{9,10,23} experiment had good coverage from 50 kHz up to 40 MHz, but suffered from internal spacecraft interference in the frequencies near 5 MHz. Also, the data were limited, since Voyager flew by quickly and observed Jupiter only from very limited sectors of local time regions of

the planet. Dependence of the phenomena on frequency or local time was difficult to determine by such observations of Voyager spacecrafts.

Genova *et al.*⁷⁸ analysing Voyager data observed that Jovian radio emission in the range of HOM and DAM are well correlated. The probability of observing non-*Io* DAM from Nancay was shown to be highly variable. These variations correspond well to fluctuations of HOM activity, influenced by the solar wind, observed by Voyager. They concluded from this result that the same source regions, at high latitudes in the Jovian magnetosphere, and the altitude extent of the source covers several planetary radii. They found no such effect for the *Io*-dependent emission, which was seen to be consistent with a source close to the field line. Galileo spacecraft as an orbiter around Jupiter observed the planet with its Plasma wave instrument at all local times¹⁵ and at frequencies up to 5.6 MHz. Still these observations helped to bridge the uncertainties in the observations made by ground based observations and Voyager spacecrafts and provided a more complete picture of the transition region. Data from the Unified Radio and Plasma Wave (URAP) experiment⁷⁹ on the Ulysses Spacecraft were used to determine the direction, angular sizes and polarization of the radio sources for remote sensing of the heliosphere and the Jovian magnetosphere. The URAP observations of Jovian radio emissions had greatly improved the determination of source locations and consequently our understanding of the generation mechanism(s) of planetary radio emissions. The study of the observed wave-particle interactions had improved our understanding of the processes that occur in the solar wind and at the Jupiter and of radio wave generation. But, the instrument to frequencies less than 1 MHz limited these studies. The hectometric (HOM) frequency exists approximately in the range $200 \text{ kHz} < f < 2 \text{ MHz}$, where as the DAM frequency range extends^{21,80} approximately from $1 \text{ MHz} < f < 40 \text{ MHz}$.

Menietti *et al.*¹⁴ analysed some of the radio emission data of HOM and lower DAM frequency range returned by Galileo during the first two Ganymede flybys (G1 and G2). They had shown that HOM emissions appear to be the low frequency extensions of DAM arcs, with source regions along either *Io* or Ganymede flux tube. While the uncertainties associated with the technique were many in practice due to the fact that the spacecraft was moving and the source regions varied in location, frequency, and amplitude with time. As a result data

analyses did not allow a precise source location, the HOM/DAM emission observed near the G1 and G2 encounters were consistent with a gyro-resonant source region with correction for refraction due to the *Io*-torus plasma to understand the results. Cassini Radio and Plasma wave instrument (RPWS)¹⁷ and the radio and plasma wave instrument (WAVES) on the WIND spacecraft⁴ in Earth orbit simultaneously observed DAM emission in the ranges from 3.6 kHz to 16.1 MHz and 1 MHz to 14 MHz, respectively. It had been revealed from terrestrial and extraterrestrial observations that occurrence probability of decametric radio emission^{24,25,81} from Jupiter within a narrow frequency range is a function of the system III (1965) central meridian longitude (CML) and the orbital position of the innermost Galilean satellite *Io* relative to the observer (*Io* phase, Fig. 7). There are four zones of CML within which the occurrence probability of the Jovian storm activity near 22 MHz is comparatively high. According to the classification of Carr *et al.*²¹, the sources are A, B, C and D. Each source consists of *Io*-related and *Io*-unrelated (non-*Io*) components according to whether *Io*'s position has a strong influence or weak or non-existent influence respectively. *Io* and non-*Io* source locations (Fig. 8) are presented in the Table 1.

Lecacheux *et al.*²⁴, Quieinnec and Zarka²⁵ and Aubier *et al.*²⁶ confirmed the source locations²¹ in the coordinate space of CML(λ_{III})-*Io* phase (Φ_{Io}). Boischoit *et al.*⁸¹ investigated the structure and the position of Jovian sources of DAM radio emission by studying

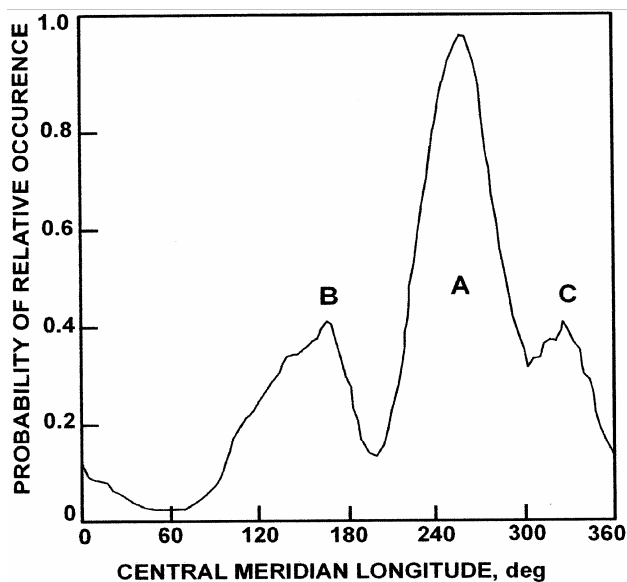


Fig. 7 — Relative probability of occurrence of DAM against central meridia longitude.[Carr *et al.*, *Physics of the Jovian Magnetosphere*, ed. A J Dessler, 1983, p.226.]

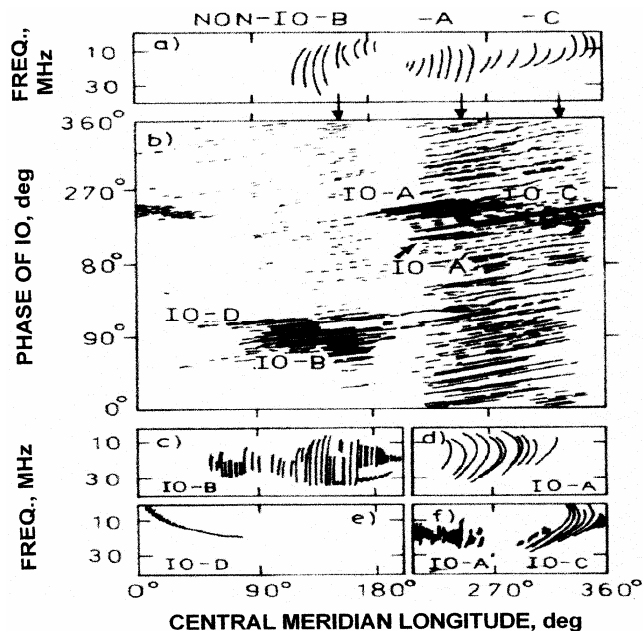


Fig. 8 — (a) Dynamic spectral behaviour of non-*Io* sources (A, B, C), (b) *Io* (A, A', B, C, D) source location in the coordinate space of *Io*-phase and Central meridian longitude λ_{III} , (c, d, e, f). Dynamic spectral behaviour of *Io* sources (B, A, D, A', C) [Carr *et al.*, *Physics of the Jovian Magnetosphere*. Ed. A J Dessler, p.226, 1983.]

Table 1 — Jovian decametric source locations in the CML- *Io* coordinate space

Source designation	CML (λ_{III}) range, deg;	<i>Io</i> -phase (Φ_{Io}), deg
<i>Io</i> -A	180°-300°	180°-260°
<i>Io</i> -B	15°-240°	40°-110°
<i>Io</i> -C	280°-60°	200°-260°
<i>Io</i> -D	0°-200°	95°-130°
non- <i>Io</i> -A	200°-300°	0°-360°
non- <i>Io</i> -B	80°-200°	0°-360°
non- <i>Io</i> -C	300°-360°	0°-360°
non- <i>Io</i> -D	0°-200°	0°-360°

the interplanetary scintillations (IPS) using broad band dynamic spectra obtained at Nancay between 15-40 MHz and arrived at the conclusion that *Io* and non-*Io* emissions are radiated, at each frequency, by very small sources in a very thin hollow conical sheet at large angle to the magnetic field lines. According to them the sources are spread spatially with frequency. They also observed that there was no preferred line of force involved in the non-*Io* emission, and as a result they inferred that electrons do precipitate all the time at every longitude, approximately near the L-shells corresponding to the orbit of *Io*. Also, *Io* in its motion interacting with that electron enhances the emission

from an extended region around the *Io*-flux tube (IFT). The emission anisotropy of the regions of different sources had been explained as evidence of the beaming of Jovian decametric radiation from the local magnetic field. Geometry of A, B, and C, D actually correspond to only two physically distinct source regions, each viewed along one side or the other of their widely opened beaming pattern. The observed dominant right-hand polarisation of *Io*-A and *Io*-B emissions thus suggested later by Kaiser *et al.*⁸², that they originated from a source region in the northern hemisphere, while left hand polarization of *Io*-C and *Io*-D emissions favour a southern hemispheric sources. Northern and Southern hemisphere emission has been separated by their polarisation, but, this is valid only for the higher frequency emissions, for frequencies below 15 MHz the polarisation is more mixed⁸².

Genova and Aubier⁸³ detected in their 3.5 months of observing only 26 cases of unambiguous left-handed-polarized emissions. The emissions correspond to two different particular patterns in the CML- Φ_{Io} diagram, corresponding to the *Io*-D and *Io*-C regions of occurrence. The measurements showed that the left-hand emissions reach lower maximum frequencies than the northern emissions, which indicate the asymmetries in the Jovian southern and northern magnetic fields. Queinnec and Zarka²⁵ combining data coverage of the range 1-40 MHz from the Waves experiment on the Wind Spacecraft and from the Nancay Decameter Array studied arc shapes over the entire frequency range (3-37.5 MHz) and revealed that *Io*-B and -D sources were observed when *Io* was near Jupiter's dawn limb (as viewed from the Earth), while *Io*-A and *Io*-C sources correspond to the dusk limb. Poquérousse and Lecacheux⁸⁴ gave first evidence of a narrow beaming of DAM emission by analysing simultaneous observations, from Nancy observatory and from space (French Soviet Experiment Stereo-5 aboard Mars 5 spacecraft). Voyager spacecrafts PRA team analysing the frequency-time (*f-t*) dynamic spectrum^{9,10} discovered that most of the Jupiter's DAM emissions in the range from a few to 40 MHz are organized into thin arc-like structures.

Dulk²² and Piddington⁸⁵ introduced a hollow cone beam model and interpreted the phenomenology of *Io*-related source A (*Io*-A) and source B (*Io*-B) emissions. Assuming a tilted dipole magnetic field and an emission cone half angle of 79°, Dulk²² established that the two CML regions for which parts

of the hollow cone beam aligned with Earth are at source A and B longitudes. Dulk²² was able to account in a rough way for the active *Io* phase regions for *Io*-A and *Io*-B emission by assuming the observed emission for closer proximity of *Io* near the cone apex longitude. Basic elements of the Dulk²² beam model have been utilised in most subsequent attempts to model the *Io*-related emission^{33,86-88}. Dynamic spectral plots of the broad band radiation received by the two Voyager space craft showed that decametric storms typically consists of multiple groups of nested-arc-like structure^{9,23,63,65-67,69,75-77}. Some authors proposed models in which each spectral arc resulted geometrically from the rotation of families of hollow cone beams of different frequencies threaded by an activated flux tube^{9,67,83,89,90}.

Maeda and Carr⁹¹ identified instances in which the ground stations and both Voyager spacecrafts recorded the same emission event from non-*Io* A storms. They demonstrated that the events were due to rotation of a continuously emitted curved-sheet beam of radiation, which could be approximated by a limited sector of a hollow cone and that the source of emission in each case was located at northern auroral zone latitudes. Maeda and Carr⁹² further analysing two spacecrafts' observations of the same spectral arc events over wide frequency range together, found that the beams of the *Io*-related sources, *Io*-A and *Io*-B (as well as non-*Io*-A) could be approximated by a hollow cone sector. Boischoit *et al.*²³ noted that in many storms there was a single arc that was distinguishable from neighbour arcs by its higher intensity and characteristic shape. Riddle⁶⁶ suggested that this principal arc was directly related to the flux tube passing through *Io*. It was implicit in Riddle's conclusion that *Io* somehow stimulated the other arcs in the vicinity in a less direct manner than the principal arc. Maeda and Carr⁶⁵ observed that in most *Io*-A storms a principal arc could similarly be identified, more on the basis of higher intensity than distinctive shape. From the Queinnee and Zarka's²⁵ analysis of *Io* controlled DAM arcs, it revealed that *Io* arcs, especially *Io*-A, -B, -C and -D arcs have a well defined structure in the frequency-time plane (Fig. 9) and lasts for hours. From their work it had been seen that *Io*-A, -B, -C and -D sources reveal different morphologies:

- (i) The *Io*-A emissions are not an isolated arc as *Io*-B, -C and -D sources but rather a series of a few (5-7) individual negatively drifting arcs [Fig. 9(c)], lasting a total of 2-hours. Their

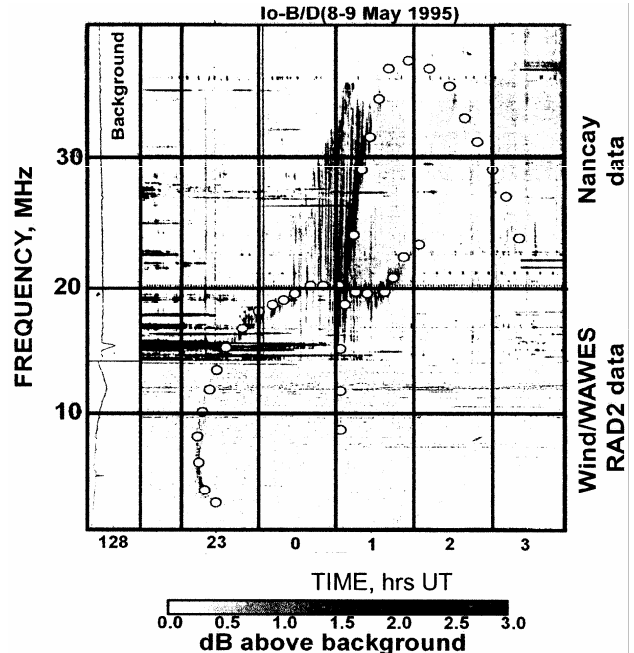


Fig. 9(a) — Dynamic spectra of *Io*-controlled arcs over the whole frequency range recorded in the combined WIND spacecraft and Nancay Dam array data recorded on 8-9 May 1995: top: *Io*-B arcs ($f_{\min} - f_{\max} \equiv 8-37$ MHz; $\langle \text{Intensity} \rangle \sim 7-13$ dB, RH – polarized) between 0000-0250 hrs UT; bottom: *Io*-D arcs ($f_{\min} - f_{\max} \equiv 3-23$ MHz; $\langle \text{Intensity} \rangle \sim 7$ dB, LH – polarized) between 2240-0140 hrs UT [Horizontal lines – man-made interference (fixed frequency), Vertical lines – Nancay data calibrations or radio emissions from terrestrial lightning. Adapted from Queinnee and Zarka, 1998]

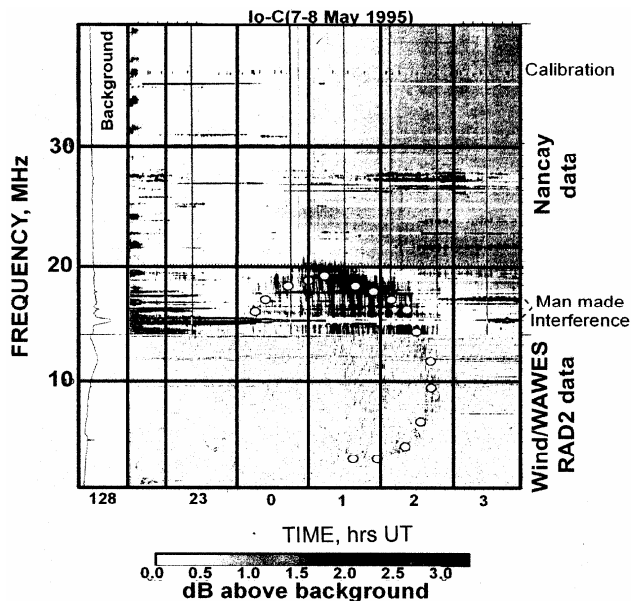


Fig. 9(b) — Dynamic spectra of *Io*-C arcs over the whole frequency range recorded in the combined WIND spacecraft and Nancay Dam array data recorded on 7-8 May 1995: ($f_{\min} - f_{\max} \equiv 3.5-20.5$ MHz; $\langle \text{Intensity} \rangle \sim 8$ dB, LH – polarized) between 2310-0110 hrs UT [same as in Fig. 9(a)]

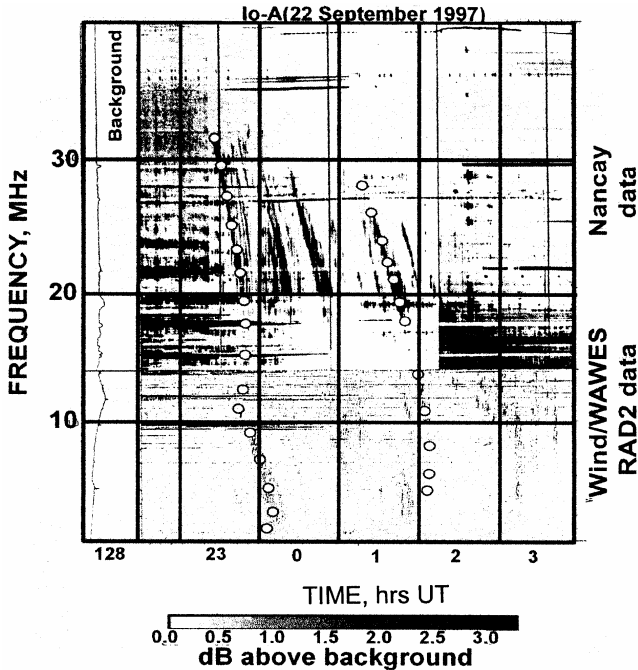


Fig. 9(c) — Dynamic spectra of *Io*-A arcs over the whole frequency range recorded in the combined WIND spacecraft and Nancay Dam array data recorded on 22 Sep. 1997: ($f_{\min} - f_{\max} \equiv 2$ –31 MHz ; $\langle \text{Intensity} \rangle \sim 7$ dB, RH – polarized) between 1940–2140 hrs UT [same as in Fig. 9(a)]

intensity is -7 dB above the back ground (in Nancay data).

- (ii) The *Io*-B arcs are made of a broad band fringe-like pattern. The *Io*-B arcs with high sensitivity reveal an “inverted U” shape [Fig. 9(a) – top spectra], with an intense positively drifting part (main arc) with fluxes up to > 10 dB followed by a much weaker negatively drifting arc (late arc) with intensity -10 dB.
- (iii) The *Io*-C arcs have an opposite curvature (“Vertex late”) with mirror-C shape [Fig. 9(b)] including weaker arcs nested inside the main one and intensity > 7 dB.
- (iv) The *Io*-D emissions appear as an isolated arc, so called “Vertex early” [Fig. 9(a)- bottom spectra]⁸³ with complex high frequency morphology.

Genova and Aubier⁹³ studied the dynamic spectra (Fig. 10) recorded by Voyager spacecrafts PRA experiment. They analysed two components of the emissions, greater and lesser arcs⁹⁴, which were seen above and below 15 MHz, respectively and observed *Io*-B, -A, -A' and -C events and the non-*Io*-B, -A and -C events. They also showed that the high frequency cut-off of the sources of non-*Io* and the *Io* emissions

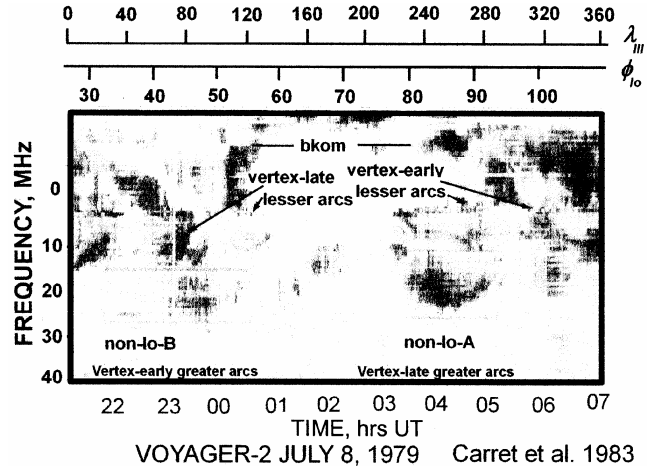


Fig. 10 — Dynamic spectrum of Jupiter’s decametric radio emissions (*Io* and non-*Io* both with vertex early and vertex late features) as observed by Voyager: it is characterized by a complex, highly organized structure. It depends on Jovian longitude, and *Io*-phase. [In the diagram, poor spatial resolution, but good spectral resolution. Carr *et al.*, 1983]

were not very different. According to them the high frequency (~ 25 MHz) radio source region is located at high latitudes. From their analysis they were not able to identify the exact position of the source region of the non-*Io* emissions. They predicted that the radiation could be produced along field lines, intersecting *Io*’s orbit at higher latitudes than the foot of the *Io*-field lines, mainly in the region magnetically connected to the magnetospheric tail⁹⁵, which could be consistent with the fact that the non-*Io* emissions, and not the *Io* ones, were subjected to the influence of the solar wind³⁵⁻⁴⁸. The location of a source on a field line linked to the magnetospheric tail can be verified from the local-time effect on the non-*Io* emissions. This phenomenon was verified by Barrow³⁹ and also by Bose and Bhattacharya⁴⁵⁻⁴⁸ and the phenomenon had been supported by Menietti *et al.*⁵⁰ from the Galileo data.

Menietti *et al.*¹⁵ analysed the radio emission data from the plasma wave high frequency receiver (101 kHz $< f < 5.6$ MHz), which included hectometric (HOM) and lower DAM frequency range, returned by Galileo during the first two (G1 and G2) Ganymede (Jovian – satellite) flybys to determine the spin plane direction to apparent source locations of the radio emission in the Jovian environment. They came to the conclusion from their analyses that both the *Io* and Ganymede flux tubes are possible source regions of the HOM/DAM arc signatures. They first identified from their analyses that Ganymede had the expected orbital phase for the vertex-early arc curvature in the

dynamic spectrum of lower frequency range of HOM/DAM radio emission. Also they showed that HOM/DAM arcs all appear to propagate from high latitudes of Jupiter, consistent with gyro-resonant source regions. Besides, they also identified some statistically significant events from the source regions at a lower or higher altitude than required for a gyro-resonant source. They interpreted such events due to refraction from asymmetries⁹⁶⁻⁹⁸ in the *Io*-torus or from source regions requiring an alternative free energy electron beams source.

The authors analysed the probability of occurrence of non-*Io* Jovian decametric radiation (NIJDR) at different solar conditions. In an 11-year solar cycle it was seen that polar coronal whole size (PCHS) changed with solar conditions. In the Jovian local time (JLT), scale occurrence probability of NIJDR varied linearly with PCHS. The above observation led to the fact that the high correlation of occurrence probability with PCHS might be due to the interaction of Jupiter magnetosphere with solar wind. It is known that IMF lines originated from sun carry the solar charged particles and, with the rotation of sun the IMF sweeps different planetary magnetosphere through different sectors. So, attempts were made to examine the phenomena of different sector boundary crossing the Jupiter's magnetosphere. Though the data of sector-boundary crossing had been recorded at 1 AU, the authors extrapolated the data to 5.2 AU, considering the fact that the structure was stable in the solar planetary frame. The analysis showed that in local time frame occurrence probabilities from different sources at different frequencies were more when IMF sector boundary crosses Jupiter's magnetosphere. At 11.4 hrs JLT non-*Io*-A source emitted radiation, whereas non-*Io*-B at 11.7 hrs JLT and non-*Io*-C did not show such distinctive feature. In this context the recent observations of Gurnett *et al.*⁴⁹ might be mentioned here. They reported simultaneous observations using the Cassini and Galileo spacecraft of radio emissions of non-*Io* origin in the frequency range from 0.5 to 5.6 MHz and extreme ultraviolet auroral emissions from Jupiter. It is revealed from their results that both of these emissions were triggered by interplanetary shocks propagating outward from the Sun. When such a shock arrived at Jupiter, it seemed to cause a major compression and reconfiguration of the magnetosphere, which produced strong electric fields and therefore electron acceleration occurred along the auroral field lines, similar to the processes that occur during geomagnetic storms at the Earth.

3.2 Evidence for beaming and cone half angle

Poquérusse and Lecacheux⁸⁴ gave first evidence of a narrow beaming of DAM emission. Voyager spacecrafts PRA team analysing the frequency-time ($f-t$) dynamic spectrum⁹⁻¹¹ observed that most of the Jupiter's DAM emissions in the range 1.3-40 MHz were organized into thin arc-like structures, lesser arcs below 15 MHz and greater arcs at higher frequencies. Kaiser *et al.*¹⁷ identified Jovian non-*Io* DAM arc beams that simultaneously illuminated both Cassini and Wind spacecrafts and they clearly classified non-*Io* A and B arcs. Also the results supported the presence of both the senses of curvature at nearly all longitudes for non-*Io* emissions as observed by Leblanc⁶⁹. Kaiser *et al.*¹⁷ had shown that hollow cones had their vertices along a Jovian magnetic field line rotating with the planet's period of 9.92 hours, or along a flux tube threading through the satellite *Io* and rotating with a period of 1.77 days. The altitude of the hollow cone along the field line or flux tube is fixed where the extraordinary (X) mode cut-off frequency equals the radiation frequency. As the flux tube or field lines co-rotates past the observer, radiation from cone walls will pass by the observer, who will see the arc-like structures in the dynamic spectrum. Arc-like structures in Jovian Dam spectrum can be realized when the leading wall of the cone passes [Vertex early or open parenthesis "("] and then when the trailing wall passes [vertex late or close parenthesis ")"] (Fig. 11). Lecacheux *et al.*²⁴ studied two *Io* controlled events, each one as a composition of two dynamic spectra recorded at Nancay (in a bandwidth 40-14 MHz) and by Wind/WAVES experiments (14 MHz to 1 MHz) to evaluate the beam geometry in the frame of available models and usual assumptions in the emission mechanisms. Now it is widely accepted that the Jovian decametric arcs are caused by the rotation past the observer of a thin curved sheet beam, which is approximately in the form of a hollow cone.

There is a systematic variation of cone opening angle with respect to frequency^{67,99}. The alternative possibility was that the emission was broadly beamed such that both spacecraft were within the beam at the same time, and that the observed arc structure resulted from a frequency-dependent time variation of the intrinsic source intensity rather than from the sweeping of a narrow frequency-dependent beam of constant intensity across the observer. If arcs were the results of intrinsic source intensity variations, the propagation-corrected arc centroid time for Voyager 1 would be the same as that for Voyager 2 at every

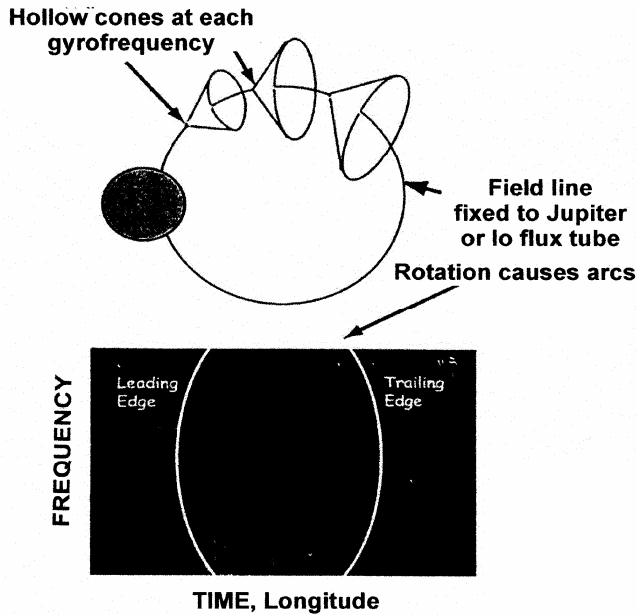


Fig. 11 — Represents the confinement of emission to the walls of the cone [The vertex of each cone on the planetary field line is at extraordinary cutoff frequency which is essentially the same as the electron gyrofrequency ($= eB/2\pi mc$, B – magnetic field strength at the vertex of the cone, e – the electronic charge, m – mass of the electron, c – velocity of light). A pair of arcs is observed in the frequency-time plane, with the leading wall of the cone causing a “vertex early” (or open parenthesis “(”) arc and the trailing wall causing a vertex late (or closing parenthesis “)”]

frequency. On the contrary, if the arc structure were due to the rotating frequency dependent hollow cone beam, the corrected arc centroid times for each frequency would be different at the two spacecraft. It is seen from Fig. 4 that the later is the case. Two curves for Voyager 1 and Voyager 2 are sharply different on each of the two dates. The corrected centroid times at all frequencies above the crossover frequencies are earlier for Voyager 1 than Voyager 2. The observed arc structure could not have resulted from an intrinsic variation in source intensity. It reveals from Fig. 12 that at each frequency the radiation was emitted in a thin curved-sheet beam with different curvatures at different frequencies, its thickness being not greater than the separation between the two spacecraft (about 6°) as viewed from Jupiter. At all the frequencies above the cross-over frequency one part of the beam was aligned with Voyager 1 first, and another part of the same beam was aligned with Voyager 2.

The analysis of the results presented in Fig. 12 was same as the basic assumptions made by Goldstein and Thieman⁶⁷ in their beam model development. The assumptions were as follows:

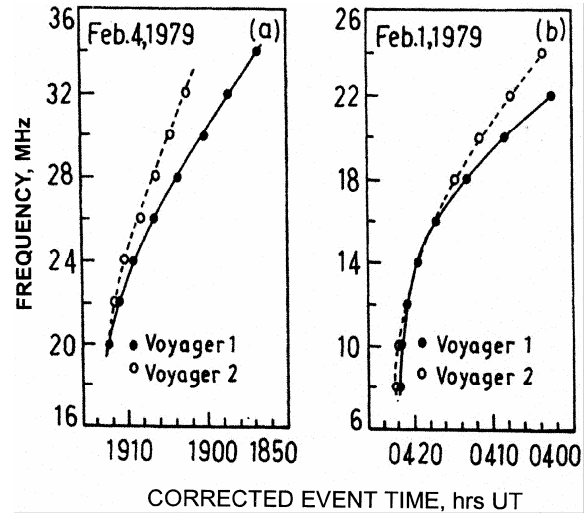


Fig. 12 — Frequency of Jovian DAM radio source versus propagation corrected event time observed by Voyager 1 and Voyager 2. [Carr *et al.*, 1983]

- (i) The curved sheet beam at each frequency is a sector of a hollow cone with its axis tangent to the *Io*-excited flux tube at the emission point, where the observed frequency is equal to the electron gyro-frequency.
- (ii) Emission occurs simultaneously at all the frequencies, continuing for time intervals longer than the durations of individual spectral arcs.
- (iii) The hollow cone-opening angle is not constant with frequency.
- (iv) The time-frequency drift pattern of the individual arc is due to the sweeping motion of the multi-cone beam pattern with respect to the observer.

As a result the alignment of the thin beams at different frequencies with the observer was at different times. It reveals from Fig. 13(a) that the multi-cone beam pattern and the time-frequency arc are due to successive cone alignments with the observer, Fig. 13(b). The sweeping of the beam pattern was for the relative motion of the *Io*-excited tube flux with respect to the observer. As shown in Fig. 12, the corrected centroid times of the Voyager 1 arc were coincident with those of the Voyager 2 arc at frequencies from 12 to 16 MHz on 1 Feb. and at about 20 MHz on 4 Feb. 1979. This clearly indicated that for all such frequencies the emission towards Voyager 1 and Voyager 2 left Jupiter simultaneously. One may assume that the radiation frequency is slightly greater than the electron gyro-frequency at the emission point and the radiation at each frequency is emitted in a thin hollow cone, the axis of which is tangential to the

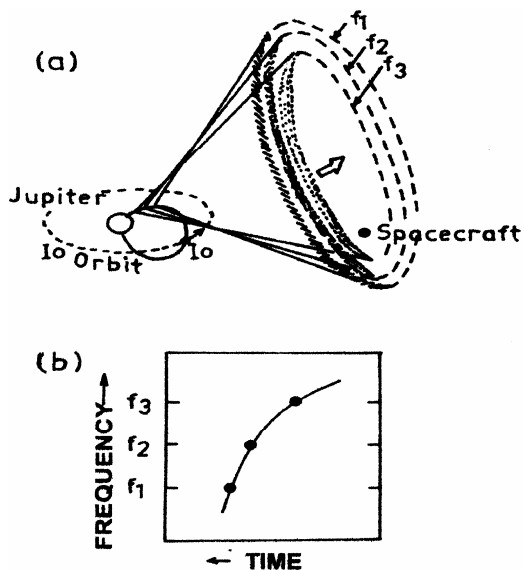


Fig. 13 — (a) Representing a schematic view of the beam-model where the source at each frequency is located in the *Io*-excited flux tube and the emitted radiation along a sector of a hollow cone. Beam cross-section at frequencies f_1 , f_2 or f_3 has been represented by shaded portions respectively; (b) frequency versus time plot [Carr *et al.*, 1983]

magnetic field at the emission point. On the co-rotating celestial sphere the cone half angle is estimated by calculating the angular distance between the station position and the position representing the field vector with the aid of the O4-field model at the source. Goldstein and Thieman⁶⁷ assumed a cone half-angle variation, in which the cone half-angle increased from the lower frequencies to the so-called nose frequency and then decreased toward higher frequencies to account for the arc structure.

Most of the authors^{83,100,101} agreed that the hollow cone half-angle could be estimated from Voyager data as between 70° and 80° . Lecacheux *et al.*²⁴ analysed the entire frequency spectrum of the Jovian DAM emission by combining the simultaneous observations in the frequency range 1-13.8 MHz from Wind/WAVES and 10-40 MHz data from Nancay Decametric Array. From the whole spectrum they selected two representative *Io*-controlled events (*Io*-B/D and *Io*-C) and analysed in terms of the available models^{22,31,67,69,85,89} of the Jovian environment. From their analyses it revealed that the *Io*-B/D event at frequencies below 20 MHz may fit the models about 87° . But they were unable to explain the *Io*-C event with the existing model of beam geometry. As a result they proposed that the departure from the theory could be resolved, provided the existing maser-cyclotron theory could accept the wave propagation

effects, occurring close or inside the radio source region, since the *Io*-DAM source follows the motion of *Io* surrounding which the magnetic field topology is complex. Under the above concept they arrived at the conclusion that the source altitude, the principle curvatures of the reflecting surface as well as orientation of the radiated beam with respect to this surface, were continuously changing functions of the active field line position.

The emission beam in some cases could even suffer substantial refraction when directed towards the reflecting surface, implying different kinds of intensity modulations like edge effects or interfering phase paths and all of these considerations might help to resolve the said discrepancy and unexplained feature. They observed the phenomena both at higher frequencies as well as at frequencies below 3 MHz, where the refraction effects might occur in the *Io*-plasma torus as suggested by them. Jovian emission mechanism theories^{72,102} predicted that hollow cone radiation beam emissions should be confined to the thin walls of the cone. As a result hollow cone arc theories demanded the measure of the thickness of the cone walls for interpreting the dynamic spectrum. Most workers have considered the duration of a given arc as a measure of its thickness. It is possible to observe an arc simultaneously (after correcting light travel time difference) by two spacecrafts, provided their angular separation as observed from Jupiter is less than the cone wall thickness. However, if the angular separation of two spacecrafts is greater than the wall thickness, then it is not possible to observe the arcs simultaneously by the spacecrafts, but will be delayed by the amount of time it takes for the cone attached to a Jovian magnetic field line or *Io*-flux tube to rotate through the angle after correcting for light travel time.

Kaiser *et al.*¹⁷ carried out Stereoscopic Radio observations of Jupiter by Cassini and Wind/ WAVES RAD2 spacecraft during two intervals in 1999. First in the month of January'99, when the Jovian longitude difference between two spacecraft was about 5.4° apart, and second, in the month of August-September'99 the angle ranged from 0° to about 2.5° . With these separations, the instantaneous widths of the walls of the hollow conical radiation beams of some of the DAM arcs were measured, suggesting that the typical thickness of the hollow conical beam was about 1.5° with an uncertainty of about 0.5° . This result supported the findings of the previous workers^{23,25,63} who got such result by analysing the

data based on the duration of a given arc at a single frequency and equating it either to the *Io*-flux tube (IFT) period^{25,63} or the Jupiter's rotation period²³. Observations of Kaiser *et al.*¹⁷ showed that the arcs were associated with *Io* or IFT, which were rotating at a slower rate than that of the Jupiter's rotation period. Though Kaiser *et al.*'s¹⁷ result supported that of the previous worker's^{23,25,69} result, but they were hesitant to conclude that the thickness of all arc cone walls is 1.5°, as they observed small number of events with Cassini-Wind spacecrafts. Hence, they suggested the possibility that the thickness might be a function of refraction in the immediate source region, and this might well vary from one location to the next. They also expected that their observations and suggestion might be verified with the planned solar terrestrial rotation observatory (STEREO) mission (launch in 2005).

Zarka *et al.*¹⁰³ proposed that statistical information about the beaming of Jovian radio components might also be estimated at each frequency by comparing the emission intensity integrated over the beam to that averaged over the complete rotation using the relation:

$$\frac{\int_{S_0}^{\infty} S \times N(S) \times dS}{\int_{S_0}^{\infty} N(S) \times dS} \dots (1)$$

where, S is the distribution of intensities at a certain frequency above a given threshold (S_0) and $N(S)$ the distribution of intensities. Zarka *et al.*¹⁰³ compared their result with the result of Kaiser *et al.*¹⁷ multiplying by 2 to take into account the two sides of the cone during one Jovian rotation. Zarka *et al.*¹⁰³ justified the remaining difference by considering the longitudinal extents of the sources of the observed components.

4 Different important features of Jovian decametric dynamic spectra

In the dynamic spectra of Jovian decametric radio emission the most commonly observed components are the long (L) bursts which are seen in the range from a few tenths of a second to a few seconds. Study of the dynamic spectra of DAM emission with high-resolution spectrograph reveals the existence of many micro features, e.g. the short (S) bursts¹⁰⁴⁻¹⁰⁷, the modulation lanes^{108,109}, the arc structure^{10,23,110} in the spectra besides the L-bursts. Warwick¹¹¹, Riihimaa¹¹²,

Warwick and Gordon¹¹³ pointed out another class of fine structured emission called narrow-band events.

4.1 L-bursts

Riihimaa¹¹⁴ observed dynamic spectra of Jupiter's L-burst with high resolution radio spectrograph of operation range close to 21-23 MHz and sensitivity ~ $10^{-21} \text{ Wm}^{-2} \text{ Hz}^{-1}$, from 1963 to 1977 in the Nancay observatory. He recorded the storms from *Io*-A, -B, -C, Non-*Io*-A, -B, -C and observed that the L-bursts (Fig. 14) could be characterized by their emission envelopes. The duration of envelopes varied from one to a few seconds, increasing towards the opposition of Jupiter to reach a maximum in the vicinity of 10-20 days before and after opposition. Modulation lanes appeared within the emission envelopes. The magnitude of the frequency (f) versus time (t) slopes of lanes was determined by CML of Jupiter, and partly by the longitude of *Io*. The sign of the slopes depended on CML only. The same types of observations were also recorded with fixed frequency spectrograph by Douglas¹¹⁵, Douglas and Smith¹¹⁶, Slee and Higgins¹¹⁷. They indicated that the interplanetary scintillation might be the cause for the one second components of the Jovian DAM bursts. The L-bursts are most commonly observed in the dynamic spectra of Jovian DAM emission, where as the S-bursts accounts for a relatively small fraction (10%).

4.2 S-bursts

Kraus¹¹⁸ reported first the existence of groups of very short (S) pulses in the Jovian DAM emission. The duration of such pulses varies from 200 ms to 1ms and such pulses were later called S-bursts (Fig. 15). The spectra of such pulses in frequency range 18-23 MHz were studied by Riihimaa¹¹² and also by Ellis¹⁰⁴ in the range 8-17 MHz. Baart *et al.*¹¹⁹ and Barrow and Bart¹²⁰ observed the S-bursts from *Io*-B and -C sources. Riihimaa¹⁰⁵ confirmed statistically the above observations in the range 18-23 MHz. He classified the S-bursts that appeared in the Jovian DAM dynamic spectra as shown in Fig. 16. Riihimaa assigned a small alphabet to each type of structure to distinguish one S-burst from another. The analysis of Riihimaa structure¹²¹ occurrences in S-patterns^{122,123} showed that more than 70% of the bursts were similar to the types a, b, e/f and g/h on an average constant frequency duration of 15 ms. The negative drift rate was found nearly similar to -31 MHz-s^{-1} . Boudjada *et al.*¹²⁴ analysing Riihimaa structures e.g. type q or type n and some times

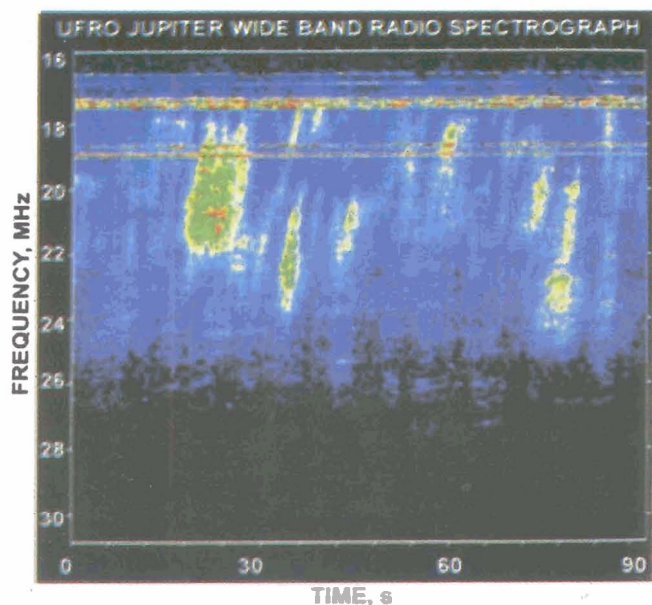


Fig. 14(a)—Dynamic spectrum of Jovian *Io-A* (L-burst) decametric radio emission recorded on 9 Aug. 1998 at 8 h 36 m 20 s UT [The emission consisting of L-bursts with the features – (i) Spectrum structures – complex, The intensity of the bursts is modulated by irregular-shaped structures drifting from high to low frequencies, (ii) polarization of emission – almost pure RH circular, (iii) Horizontal lines at a constant frequency are radio station interference. ufro1.astro.ufl.edu/lo-B.htm]

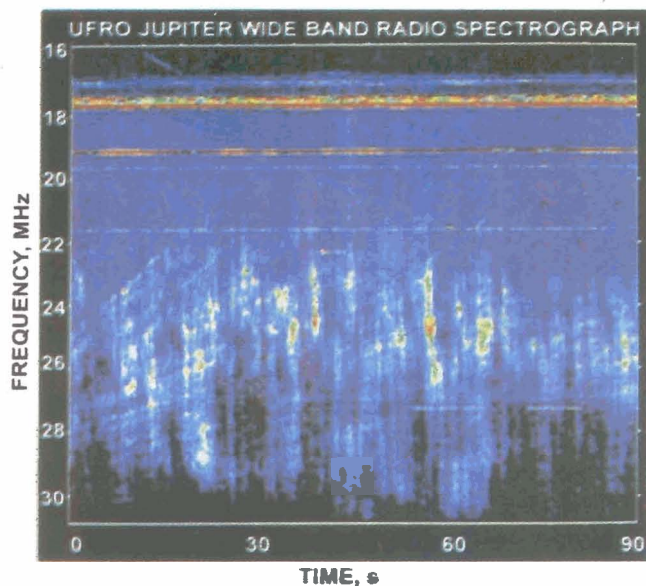


Fig. 14(c)—Dynamic spectrum of Jovian *Io-B* (L-burst 2) decametric radio recorded on 9 June 1998 at 11 h 12 m 50 s UT [The emission, consisting of L-bursts with the features – (i) frequency range – 20-31 MHz, (ii) structures – two sets of drifting features, (a) the low frequency drift about 180 kHz/s; (b) the high frequency drifts – about 60 kHz/s, (ii) polarization of emission – RH elliptical; (iii) the diagonal deflection is a sweeper station [Horizontal lines at a constant frequency are radio station interference. ufro1.astro.ufl.edu/lo-B.htm]

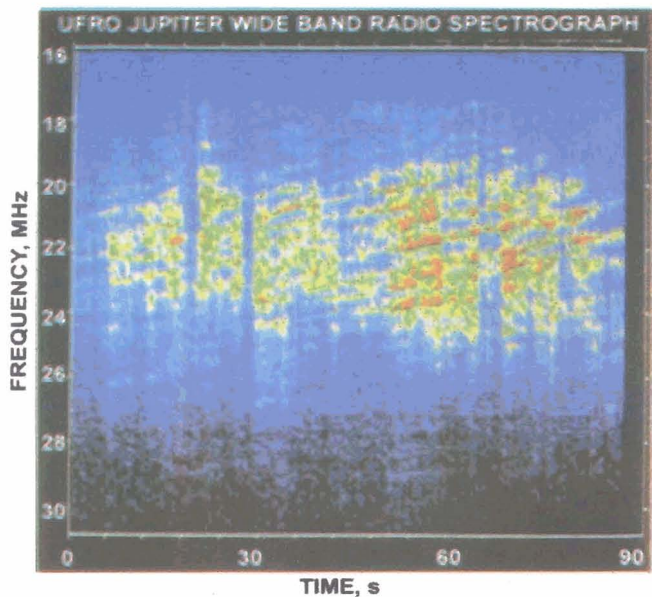


Fig. 14(b)—Dynamic spectrum of Jovian *Io-B* (L-burst 1) decametric radio emission recorded on 20 June 1997 at 10 h 12 m 50 s UT [The emission, consisting of L-bursts with the features – (i) frequency range – 17-27 MHz, (ii) structures – drifting from high to low frequencies at about 40 kHz/s are present; (iii) polarization of emission – RH elliptically; (iv) the faint horizontal line – about 27 MHz is radio station interference. ufro1.astro.ufl.edu/lo-B.htm]

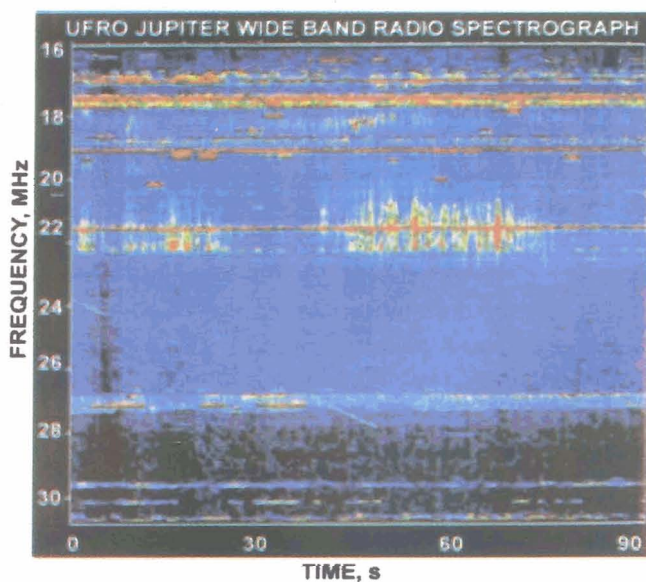


Fig. 14(d)—Dynamic spectrum of the Jovian *Io-C* (L-burst) decametric radio emission recorded on 15 June 1998 at 11 h 50 m 40 s UT [The emission, consisting of L-bursts with the features – (i) frequency range – 18-22.5 MHz; (ii) polarization of emission – LH elliptical; (iii) the diagonal deflection is a sweeper station. Horizontal lines at a constant frequency are radio station interference. ufro1.astro.ufl.edu/lo-B.htm]

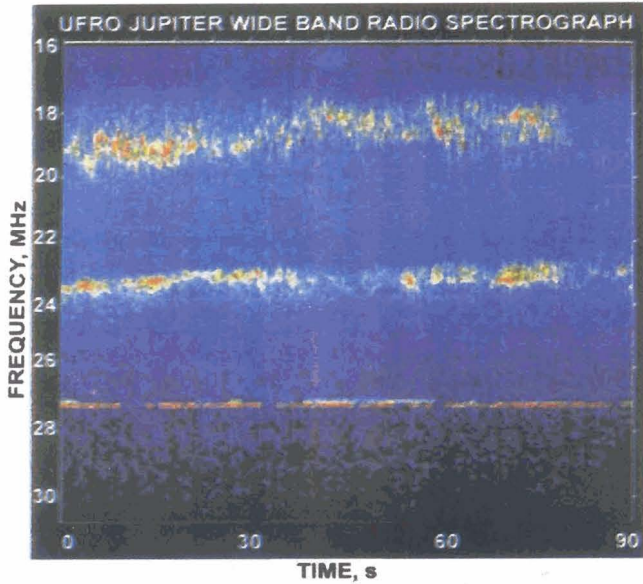


Fig. 15 — Dynamic spectrum of Jovian decametric *Io*-B (S- and L-bursts) radio emission recorded on 6 Sep. 1997 at 4 h 33 m 40 s UT [Two bands of emissions are present. Upper spectra – the low frequency band consists of *S*-bursts; Middle spectra – the high frequency band consists of narrow band L-bursts; Lower spectra – the horizontal lines at around 27 MHz are Citizens Band (CB) radio stations. ufro1. astro. ufl. edu/*Io*-B.htm]

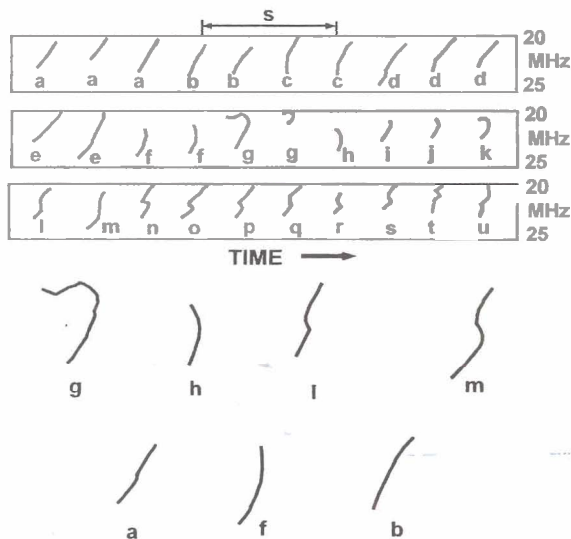


Fig. 16 — Dynamic spectra of Riihimaa classified *S*-bursts from a catalogue of observations made in Oulu (Finland) from 1974 to 1989 [The drift rate $\sim \pm 25 \text{ MHz s}^{-1}$ with a frequency band width 3 MHz. adapted from Boudjada *et al.*, 2000]

partially recorded type *f* or type *a* more precisely showed (Fig. 17) that individual *S*-bursts of those types were composed of three parts (by decomposing these into *R*-up, *R*-center and *R*-down). Both bursts (L- and *S*-bursts) could occur in the same storm, where a transition from L- to *S*-bursts was observed

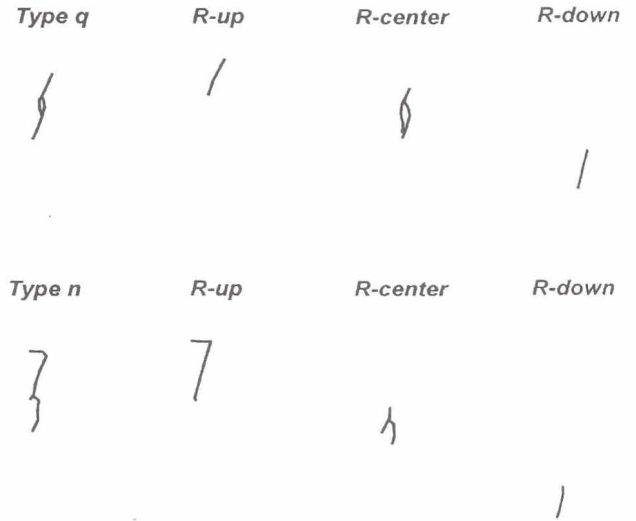


Fig. 17 — Decomposition of *q*-type and *n*-type *S*-bursts into *R*-up, *R*-center and *R*-down parts [adapted from Boudjada *et al.*, 2000]

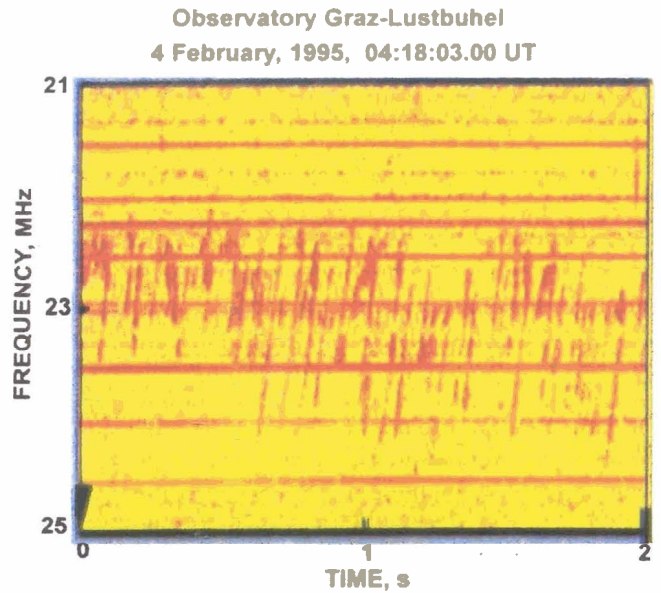


Fig.18 — Presents high resolution dynamic spectra of Jovian *S*-bursts recorded in the Graz-Lustbuhel observatory [Each pixel has time and frequency resolution of 4 ms 20 kHz, Colour coded intensity range: (i) yellow: -115 dBm , (ii) -65 dBm , the average drift rate is -20 MHz . Adapted from Rucker *et al.*, 1992.]

followed by a return to L-burst^{107,122,125}. It had been observed¹²⁴ that in the CML-*Io*-phase diagram, there were two high probability regions of Jovian millisecond radio bursts *Io*-B and -C sources. In both cases positions of the satellite-*Io* were on the edge of the planet with regard to the observer at 90° for *Io*-B and 250° for *Io*-C. An example¹²⁶ of *S*-bursts observed at the observatory Graz-Lustbuhel is displayed in the Fig. 18.

Queinnec and Zarka¹²⁷ analysed statistically the bandwidth, flux density, power, energy, and polarization of Jovian S-bursts from high-resolution observation performed in Nancay using an acousto-optical spectrograph. From their observations it revealed that the S-burst flux density were found to follow a power law distribution with an average index -2 , with an average rated power of 10^9 W subject to sudden variations at a time scale of minutes. The density of S-burst occurrence in the $f-t$ plane was found to be ~ 0.3 . The average flux density normalized at 1 AU was $4 \times 10^{-20} \text{ Wm}^{-2}\text{Hz}^{-1}$ and observed S-bursts corresponds to dominant right-hand elliptical polarization. Spectral variation of this polarization ratio was suggested by the observation, whose interpretation in terms of radio beaming angle was also consistent with earlier studies. They observed that S-bursts were polarized mainly with right-hand polarization, but the ratio of the right- and left-hand polarization¹²⁸⁻¹³⁰ varied from storm to storm. Rucker *et al.*¹³¹ analysed in depth the microstructure inherent in the S-bursts by means of the newly developed waveform receiver and connected to the decimeter of the world's largest radio telescope UTR-2 (Kharkov), which yielded waveform measurements of Jovian S-bursts, which had been analysed by wavelet analysis method. The outcome of their investigation was the detection of clear signatures of micro second (μs) modulations, providing the evidence of a superfine burst structure with the following parameters:

- (i) Instantaneous frequency band of one separated μs pulse of 100-300 kHz,
- (ii) Time duration of one separated μs -pulse of 6-15 μs , and
- (iii) Time interval between closest subsequent μs pulses of 5-25 μs .

The apparent frequency drift of a millisecond burst evidently results from sequentially decreasing frequencies of subsequent sub pulses; each representing an island of phase coherent gyrating electron bunches.

Recently Ergun¹³² observed that repetition frequency of S-bursts and frequencies (~ 20 Hz) of the eigenmodes of inertial Alfvén waves in Jupiter's upper ionosphere are somehow related. Inertial Alfvén waves accelerate electrons with fluxes that are modulated at Alfvén wave eigenmode frequencies. The modulated electron fluxes, in turn, may generate the S-Burst emissions but the exact growth mechanism has not been identified.

4.3 N-band bursts

Warwick¹¹¹, Riihimaa¹¹², and Warwick and Gordon¹¹³ pointed out narrow band events (Fig. 19) in the Jovian DAM dynamic spectra. Later on Riihimaa¹³³ studied the occurrence of N-band emission in the Io -CML diagram. He pointed out that the N-band events are relatively infrequent phenomena which occur more frequently when Io -phase in between 210° and 300° for a large range of CML (110° - 360°) and he also pointed out that the event consists either of groups of S-burst trains or of bands splitting events separated by 100-200 kHz. Riihimaa and Carr¹²⁵ described narrow band L-emission intersected by S-bursts in the range of 21-23 MHz. Boischoy *et al.*¹³⁴, Leblanc and Rubio¹³⁵ observed N-band emission at the upper frequency limit of the broad band DAM emission in a small area of the Io -B region, in the Io -CML diagram. In some cases they observed that the intensity of the upper frequency broad band is reinforced and the gap between the narrow band and broadband is constant and very regular. The splitting is observed either at the upper frequency of S-bursts or at the cut-off frequency of the broadband continuum emission. They thought such phenomenon as an emission split at the upper frequency, due to an interference or a diffracting pattern. They also noticed in the Voyager

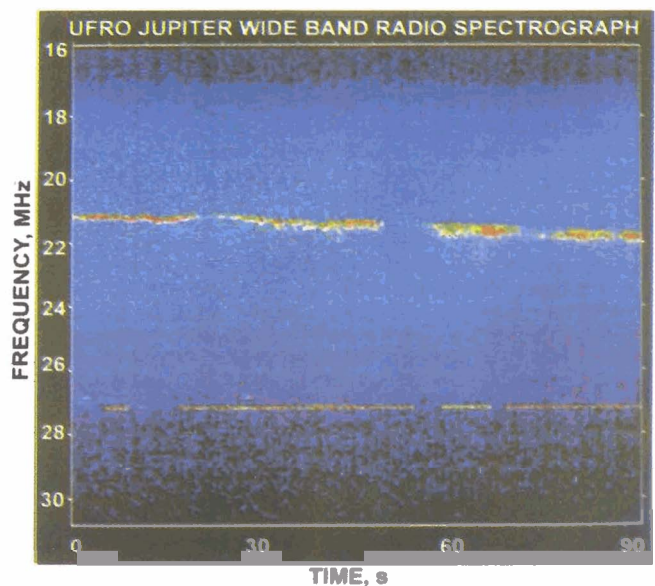


Fig. 19 — Dynamic spectrum of Jovian Io -B (N-band emission) decametric radio emission recorded on 6 Sep. 1997 at 3 h 31 m 50 s UT [The emission, consisting of N (narrow band) emission with the features – (i) Frequency range and structures drifting slowly between 20 and 22 MHz, (ii) polarization of emission – pure RH circular, (iii) the horizontal lines around 27 MHz are Citizens B and (CB) radio stations. ufro1.astro.ufl.edu/Io-B.htm]

PRA record of *Io*-DAM in the frequency range 1-40 MHz that the narrow band of the splitting is always polarized, same as in the the broadband emission. It is important to note that the splitting in the *Io*-B and -C regions are observed with R-H and L-H circular polarizations, respectively. The ratio of its bandwidth over the frequency of occurrence is equal to about 10. The splitting appears exactly similar to that observed on the high-resolution record of Nancay.

Boudzada *et al.*¹²⁴ studied the relationship between some typical S-burst events chosen from Riihimaa catalogue¹²¹ and the Jovian N-band emissions. Their analysis of the temporal evolution of the Jovian narrow band involves the presence of fine structures, i.e. the S-bursts, with short time duration of about a few tens of milliseconds. Each S-burst duration and the short time scale of the gap in the N-band account for a mechanism totally intrinsic to the radio source. Oya *et al.*¹³⁶ analysed 65 S-burst events in the dynamic spectra of Jovian DAM radiations in the period from 1983 to 2000 using high time resolution radio spectrograph with a time resolution of 2 ms and the bandwidth of 2 MHz. Within the occurrence of 65 S-bursts they identified 26 events as the S-N burst events, which are characterized by the interaction between the S-burst emissions and the N-band emissions. In the dynamic spectra of the S-N burst, emission trend with negative and slower frequency drift named as Trailing Edge Emissions (TEE), which often follows the appearance of S-bursts. A typical S-N burst phenomenon with complex features has been shown in Fig. 20. The duration time of TEE was about 0.1 s. Oya *et al.*¹³⁶ arrived at the conclusion from their analysis of the microscopic view of the dynamic spectra (Fig. 21) that there is no correlation between the drift rates of the S-bursts and associated TEE. The drift rate of the S-burst depends on the frequency, while there is no such dependence for the drift rate of the TEE. In the dynamic spectra the TEE phenomenon smoothly connected to the N-burst reflecting the fact that the center frequency, bandwidth and the drift rate of the TEE coincide with those of the N-burst at the merging point (Fig. 22). Arkhipov *et al.*¹³⁷ explained the Riihimaa classified S-bursts and N-band spectra in terms of a helical motion of radio sources with a small group velocity of emission.

4.4 Modulation lanes

It has been mentioned earlier that, since the discovery of Jovian DAM in 1955, inherently there are three types of bursts (e.g. L-bursts, S-bursts, and

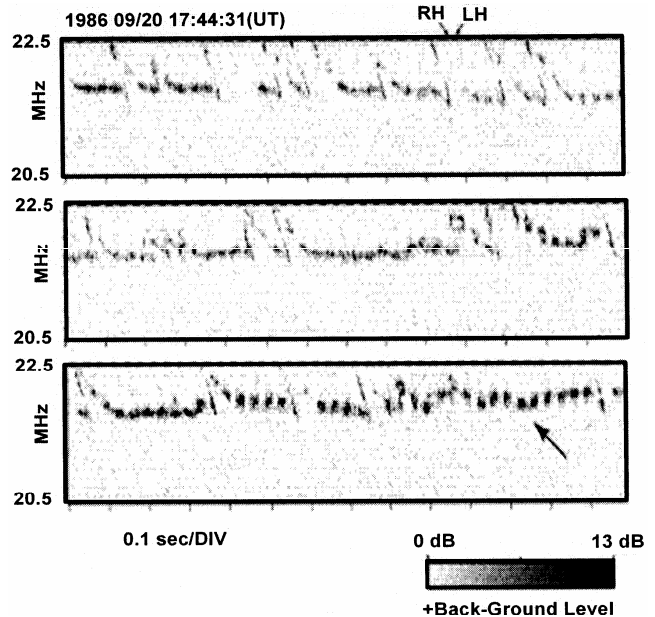


Fig. 20 — Dynamic spectrum of S-N bursts in a frequency range of 20.5-22.5 MHz recorded on 20 Sep. 1986 from 17:44:31.0 to 17:44:35.2 (UT) at Tohoku University [Nature of polarization (RH/LH) are indicated by small arrows. In the spectrum there are some periodic interruptions (shown by large arrows) due to recording system. Adapted from Oya *et al.*, 2002]

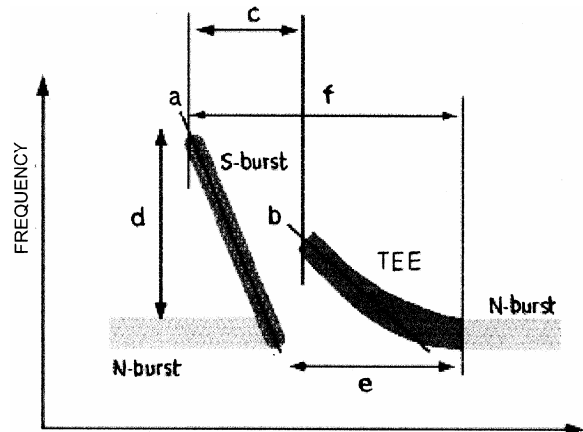


Fig. 21 — Characterization of dynamic spectra presented in Fig. 20 by the following six parameters: (a) S-burst drift rate (MHz/s), (b) trailing edge emission, (c) time interval from the appearance of S-burst to the appearance of TEE, (d) s-burst frequency range (MHz), (e) time interval of appearing N-burst after disappearance of S-burst, (f) time interval between the appearance of S-burst and disappearance of TEE (ms) [Adapted from Oya *et al.*, 2002.]

N-band events) in the Jovian dynamic spectra of DAM emission. With ground based instruments L-bursts of 1-s duration has been generally seen to be modulated by interplanetary scintillations (IPS)^{108,116,117}. Riihimaa discovered that L-bursts groups of lanes drift in the time frequency plane. This feature of drifting lanes is called modulation lanes.

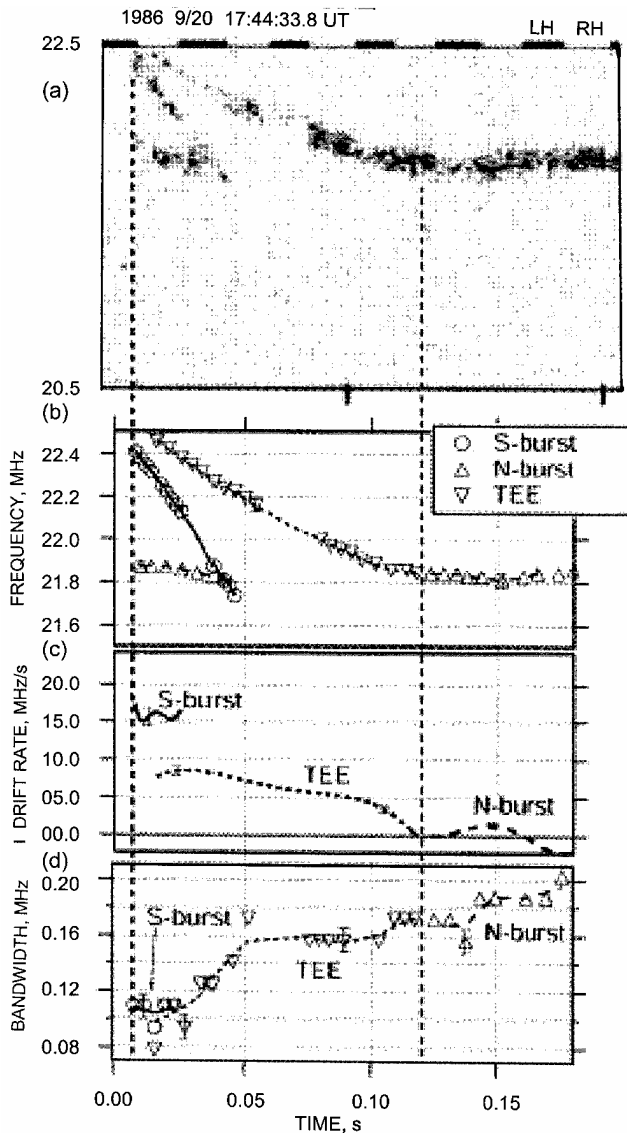


Fig. 22 —Part of the dynamic spectrum (Fig. 20) and the temporal variations (b)-(d) of the center frequency, the drift rate, and band width [Adapted from Oya *et al.*, 2002.]

Later he studied these features extensively in 20-23 MHz frequency range. Boischot *et al.*¹³⁴ and later Genova *et al.*¹⁰⁹ identified three types of Lane-like modulations in large bandwidth dynamic spectra of Jovian DAM emission with the Nancay Array. Each type has definite spectral and occurrence characteristics. The three types are: (i) terrestrial ionosphere scintillations, (ii) modulation lanes as discovered by Riihimaa and (iii) high frequency lanes.

4.4.1 Terrestrial ionosphere scintillations

The modulation of terrestrial ionospheric origin bears the following spectral characteristics:

- These types are superimposed with other usual spectral features (Arcs, IPS, modulation lanes) in the dynamic spectra.
- The whole emission frequency range are strongly modulated by this feature.
- Frequency displacement has been observed in the simultaneous records of right and left hand polarizations.
- Frequency drift and spacing of this type vary with time and frequency.

Though in most cases the variation is slow and continuous and their frequency drift can have both signs, negative drifting can be seen about 75% of the time of duration of such feature.

These types of modulations are irregular and can be observed between two sequences of smooth lanes. A typical value¹⁰⁹ of the frequency drift is $\sim 20 \text{ kHz}^{-1}$ at 20 MHz; of the frequency spacing between two lanes $\sim 0.5\text{-}1 \text{ MHz}$ of the time spacing $\sim 1 \text{ min}$. As this fringe type of phenomenon has been seen to be superimposed on the normal dynamic spectrum, it indicates that it might be originated close to the Earth, after the radio emission of Jovian origin has suffered the modulation effects close to Jupiter and in the interplanetary medium. According to Riihimaa¹⁰⁵ this type of fringes are called “broadband lanes”, the spacing of such lanes is greater than about 500 kHz. Genova *et al.*¹⁰⁹ interpreted that dynamic spectra in the DAM range of Jovian origin may suffer diffraction by semi-periodic ionospheric F-zone inhomogeneities during their passage through ionosphere and as a result, this type of features can be seen. A fluctuation in the F-zone dimension and/or velocity can give rise to the variability of different parameters. Several such ionospheric lenses may be responsible for irregular pattern of such type of fringes.

4.4.2 The modulation lanes of Jovian origin

These categories was discovered by Riihimaa¹⁰⁸ and also observed by Genova *et al.*¹⁰⁹ with Nancay Array. Riihimaa distinguished three kinds of modulation lanes in his study with Jovian dynamic spectra of DAM in the frequency range of 20-23 MHz. Genova *et al.*¹⁰⁹ observed such feature with Nancay's broadband spectrograph Array and tabulated the main properties of such lanes as follows:

- The lanes are appeared stable during 10 min to 1hour and cover the whole emission frequency range,

- (b) The curvature of L_2 and L_4 lanes are similar and their absolute drift rate decreases towards lower frequencies,
- (c) There is absence of marked qualitative difference between the two channels of circular polarization,
- (d) Their modulation depth, variable from storm to storm, is few db L_2 Lanes are observed for $60^\circ < \text{CML} < 260^\circ$ at all Φ_{Io} and particularly in the Io -B source (B_1 and B_2); L_4 lanes are observed for $60^\circ < \text{CML} < 310^\circ$ at all Φ_{Io} and in the Io -C regions (Fig. 23). L_3 lanes appear almost in the B_2 region.

4.4.3 High frequency lanes

Genova *et al.*¹⁰⁹ observed this kind of modulation for the first time. This feature tends to cover a small frequency range in the highest frequency part of the emissions and due to this feature this type of

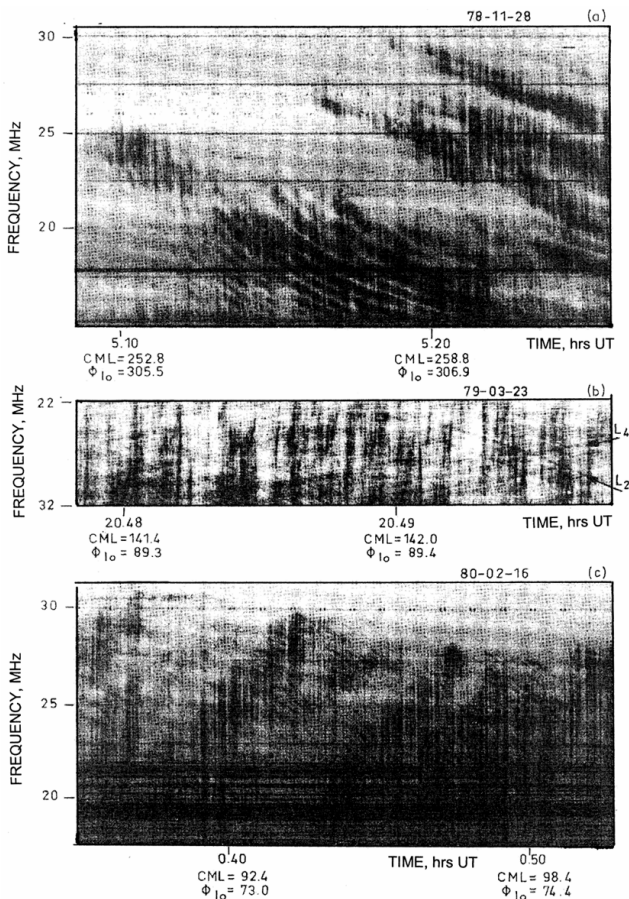


Fig. 23 — Dynamic spectra recorded at the Nancay Observatory showing three types of modulation lane: smooth ionospheric modulations-drift negatively with a large modulation depth; (b) L_3 modulation lane structure composed of L_2 positively drifting and L_4 negatively drifting lanes; The negatively drifting modulations cross over the vertex early arcs of the Io -B source spectral arcs; (c) high frequency lanes [Adapted from Genova *et al.*, 1981.]

modulation was named as high frequency (hf) lanes. These modulations are not as regular as the other two types mentioned earlier and have a small modulation depth often less than 3 dB, but they always have the same spectral characteristics. Frequency drift of such spectra is always negative within -5 and -50 kHz s^{-1} . The curvature of the spectra is opposite to that of L_4 modulation lanes and as a result the drift rate increases with frequency: the most probable value is between -10 and -25 kHz s^{-1} at 25 MHz and -5 and -20 kHz s^{-1} at 29 MHz. The characteristics and particularly the drift rate of such modulation do not show any significant variation along one particular storm. Their occurrence does not show any seasonal or local time dependence as that of terrestrial ionospheric origin, but is strongly dependent on the position in $\text{CML}-\Phi_{Io}$ coordinate system. They occur almost only in Io -B region and in another region including both Io -A' region and the low CML part of Io -A. Lecacheux *et al.*¹³⁸ proposed that the arc pattern of such spectra have its origin in diffraction by a density hole located permanently in Io -torus. Slight inhomogeneities in the density gradient on the sides of the hole might be the site of creation of such type of modulation in the arc intensities like hf-lanes. But this reason is not sufficient to explain the hf - lanes observed in Io - B source. Though Imai *et al.*¹³⁹ interpreted the DAM modulation lanes in terms of radiation scattering due to FAC inhomogeneities in the Io plasma torus, that model cannot explain lanes with opposite drifts with respect to Io torus rotation. According to the model proposed by Arkhipov¹³⁶ FAC inhomogeneities of the magnetospheric plasma above the Jovian ionosphere generate such modulation lanes.

5 Identification of field-aligned currents in the terrestrial and Jovian magnetosphere and its consequences

From a review of different characteristic features of terrestrial and jovian radio emissions, it has been revealed that in the process of emission besides the planetary magnetic field, vital roles are also played by available sources of plasma in the ionosphere and magnetosphere separately or by some coupling mechanism.

The growing awareness of the function of field-aligned currents (FAC) in magnetosphere-ionosphere coupling has allowed a conceptual framework, within which the plasma wave may be understood widely.

Barbosa *et al.*¹⁴¹ interpreted high altitude satellite data of impulsive electrostatic waves due to FACs in the context of temporal events associated with geomagnetic storms and substorms. Extensive investigations of the magnetospheric tail plasma sheet¹⁴² at high altitudes/latitudes¹⁴³ revealed the persistence of a characteristic wave mode in certain regions, where FACs were suspected to flow. This type of emission is termed as broadband electrostatic noise (BEN), has the nature of being very impulsive with large peak-to-average field ratios ($E_{\max} \sim 10$ mV/m) and extends over frequencies from 10 Hz to several kHz with power law dependence. The peak intensity occurs¹⁴² in between 10 and 50 Hz. When intensity-time profiles of the spectrum analyser are displayed, this mode can be distinguished from other magnetospheric noise by the usually sharp prominence out of the lower intensity surrounding noise (e.g. auroral hiss, etc.) and it is localized to narrow portions of the orbit when the satellite is not rapidly changing in magnetic local time. Thus the noise is confined to discrete field lines (auroral) at high latitudes or the edges of the plasma sheet in the magnetotail¹⁴². If any ambiguity occurs in the identification of BEN, the presence of magnetic noise bursts removes that doubt. Many theories described the generation of BEN to current driven instabilities of the plasma distribution¹⁴⁴⁻¹⁴⁶. They exploited the terrestrial BEN-FAC association phenomenon to the Jovian magnetospheric plasma wave events.

Matsumoto *et al.*¹⁴⁷ observed during the analysis of data from the deep magnetotail of terrestrial magnetosphere by the Plasma Wave Instrument and Comprehensive plasma Instrument on board the GEOTAIL spacecraft that it experienced multiple crossings of the plasma sheet boundary layer, BEN and Langmuir wave alternatively. The dynamic spectra are very bursty in time, and their waveforms are showing a series of electrostatic solitary waves (ESW). The ESW are observed in the presence of a hot thermal electron distribution function. Omura *et al.*¹⁴⁸ studying ESW and the corresponding GEOTAIL electron velocity distribution functions observed a series of ESW in the plasma sheet boundary layer of the Earth's magnetotail, where enhanced fluxes of high energy electrons are flowing along the ambient magnetic field.

Kasahara *et al.*¹⁴⁹ studied waveforms of BEN in ion heating region observed by Akebono and found that the waves are classified into continuous noise and impulsive noise. They showed the spatial distribution

of the continuous noise statistically dependent on local time, geomagnetic activity, and the season. They analysed intensity-time profiles of plasma wave measurements by the Voyager 1 (V1) plasma wave system (PWS) spectrum analyser having channel width from 10 Hz to 56.2 kHz. They compared the Jovian spectra with terrestrial observations and indicated eight BEN events near the edges of the plasma sheet during both inbound and outbound journey of V1 through the Jovian magnetosphere. The intensity decreases with increasing distance beyond $10R_J$, and the noise was not detected in the outer magnetosphere beyond $30R_J$. The emission below 1 kHz has shown distinctly a power law dependence ($\sim f^{-2.5}$). Gurnett and Frank¹⁴⁵ and Gurnett *et al.*¹⁵⁰ characterized terrestrial BEN having a slope of $f^{-2.2}$ and this is deemed to correspond well with the Jovian emission. This finding led Barbosa *et al.*¹⁴¹ to conclude that there is a positive evidence for FAC in the middle magnetosphere of Jupiter. Hill¹⁵¹ proposed that in the course of magnetosphere-ionosphere coupling, steady-state field aligned currents (FACs) take a vital role to mediate angular momentum from Jupiter's ionosphere into Jupiter's middle magnetosphere to spin up the radially expanding magnetospheric plasma.

Dougherty *et al.*¹⁵², analyzed the data recorded by the dual vector helium/fluxgate magnetometer flown onboard the Ulysses spacecraft during the flyby of Jupiter in February 1992 for identifying the presence of field-aligned current signatures. The data from both inbound and outbound passes show evidence of 'leading' and 'lagging' azimuthal field signatures, where the field bends out of the meridian, and which are signatures symptomatic of current systems associated with departures from co-rotation. On the outbound pass, the most intense signatures are found, where the field switches from a configuration symptomatic of the field lagging corotation to a configuration representing the field leading. The latter configuration also corresponds to a tail-like displacement of the field and, indeed, the magnetometer data alone cannot distinguish the source of the current system, which could be due to solar wind magnetosphere coupling, or which may arise from internal stress imbalance. Field-aligned current flow is expected wherever stress is being transmitted electromagnetically along the magnetic field direction. Sources of such currents at Jupiter are departures within the magnetosphere from corotation, momentum transfer from the solar wind, or

centrifugally driven magnetospheric outflow. It is pointed out that the azimuthal field component provides a simple first-order means of monitoring the presence of currents, the currents occurring in regions where the azimuthal component changes significantly.

A model¹⁵³ of the field aligned current system in the Jovian Magnetosphere, particularly near *Io*-plasma torus, was developed on the basis of two important features: (i) sheared plasma flow around *Io*, and (ii) mass injection from the atmosphere of *Io* into this motion. It is shown that the mass-momentum transfer from *Io* can produce a large enough current along the magnetic field which can generate ion-cyclotron waves. A nonlinear mechanism which generates kinetic Alfvén waves from these waves has been reexamined. It is found that the kinetic Alfvén wave generated by this mechanism can produce a sufficiently large electric field along the magnetic field to accelerate particles to a few tens of keV within a fraction of the Alfvén wave period. Thus, this model is capable of generating both electrostatic and electromagnetic waves associated with energetic electron beams, which were observed by the Galileo space craft during its passage near *Io*.

From the different spacecrafts' magnetometer data analysis it reveals that in the dusk sector near 100 R_J the configuration of the magnetic field of the Jovian magnetosphere varies with distance from the equatorial current sheet. The changing twist out of meridian planes is consistent with flows that lag corotation near the equator but that may lead corotation at higher latitudes. A portion of the field perturbation may be produced by magnetopause currents. Kivelson *et al.*¹⁵⁴ argued that the observed sheared field structure requires field-aligned current flowing toward Jupiter's ionosphere inside the magnetopause but beyond 100 R_J . This current must include a portion of the return current of the system that enforces partial corotation of outward moving magnetospheric plasma and may also be fed by boundary layer currents of the region 1 type. They analysed the data of differing field orientations observed by Galileo near the equatorial plane and those reported at higher latitudes from Ulysses for roughly 30 h in December 2000 during an interval of quiescent solar wind when the Jovian plasma sheet was displaced northward of its normal near-equatorial position, leaving Galileo in the duskside southern magnetic hemisphere for several planetary rotations. They estimated the total current into the auroral ionosphere as 6 MA, and this current would flow into

a narrow band of latitude (< 2) poleward of the main auroral oval. This estimate was found to be consistent with the shear in the azimuthal field component.

Cowley and Bunce¹⁵⁵ and Hill¹⁵⁶ correlated FACs to the main auroral oval on Jupiter. Saur *et al.*¹⁵⁷ showed that the intensity of small scale Alfvén waves maximizes on the auroral field lines. They related these spatial and temporal fluctuations in the presence of a net background current to the formation of the main auroral oval. Their concept led to a total energy in the accelerated electrons and a field aligned voltage in concurrence with the observations of the aurora oval.

Using global magneto-hydrodynamic (MHD) simulation of the interaction of Jupiter's magnetosphere with the solar wind, Walker and Ogino¹⁵⁸ investigated the effects of the solar wind on the structure of currents in the Jovian magnetosphere. In their simulation they assumed that the current sheet is weaker on dayside than the night side with some local regions where the current density decreases by more than 50 %. As a result there is a non-uniform distribution of current along the azimuth. The current sheet also contains strong radial "corotation enforcement" currents. Almost at all local times the outward radial currents are observed, but there are some regions where the direction of currents is toward the Jupiter. In the local afternoon and evening regions the current pattern is especially complex. The FAC pattern is also complex in the near equatorial magnetosphere. They simulated the currents from the inner boundary to the ionosphere and observed the expected configuration for the ionosphere to drive corotation. At lower latitudes the currents are away from Jupiter and at higher latitude the currents are towards Jupiter. The upward FACs map to larger distances on the night side (40-60 R_J) than on the dayside (20-30 R_J). They tried to observe the effect of solar wind dynamic pressure and IMF by simulation study on the structure of the currents and arrived at the conclusion that the current sheet and FAC were slightly stronger with higher pressures, but the IMF had a stronger effect on the currents with the strongest currents for northward IMF with a lag in time in responding by the magnetosphere.

Nichols and Cowley¹⁵⁹ suggested a model assuming the values of effective Pedersen Conductivity of the Jovian ionosphere and the mass outflow rate of Iogenic plasma on which the amplitude and spatial distribution of the coupling currents flow between Jupiter's ionosphere and middle magnetosphere. They

investigated the dependence of the solutions for the plasma angular velocity and current components on the parameters over wide ranges. In doing so they considered two models of the magnetosphere – dipole alone, and an empirical current sheet field based on Voyager data. The key feature of their model is that the current sheet field lines map to a narrow latitudinal strip in the ionosphere, at approximately 15° co-latitude. From their analysis it is observed that the major distinction between the solutions for the dipole field and the current sheet concerns the behaviour of the FACs. In the dipole model at moderate equatorial distances the direction of the current reverses, and the current system wholly closes if the model extends to infinity in the equatorial plane and to the pole in the ionosphere. In the approximate current sheet model, however, the FAC is unidirectional, flowing consistently from the ionosphere to the current sheet for the sense of the magnetic field of the Jupiter. In the later model current closure must then occur at higher latitudes, on field lines outside the region described by the model. The absolute values of the currents are also higher for the current sheet model than for the dipole with the same parameters, by factors of approximately 4 for the field-perpendicular current intensities, approximately 10 for the total current flowing in the circuit, and approximately 25 for the FAC densities.

The FACs at Jupiter had been inferred from radio observation²¹ of DAM emission. Jovian DAM controlled by *Io* has long been assumed to be associated with FAC resulting from the electrodynamic interaction of the satellite with the Jovian ionosphere. Barbosa¹⁶⁰ raised a question after the Voyager spacecraft findings of local time dependence¹¹ of non-*Io* DAM about the process involved in FAC generated DAM emission from co-rotation dominated *Io*-flux tube on the L-shell near $L = 6$. In this regard it is to be mentioned that *Io*-dependent emissions do not exhibit local time effects^{21,47}. As far as it is known that there has never been any evidence of spatial relation between two DAM emissions. Barbosa¹⁶⁰ showed other several FAC systems associated with iogenic plasma transport and for one of them they showed theoretically a FAC dissipative output of ~ 60 tW. He argued that the corotation breakdown region outside of $18R_J$ is more susceptible to the influence of the solar wind and dawn-dusk asymmetries of the magnetospheric configuration. They solicited that any variation of solar wind parameters is more likely

affect a FAC system in the middle magnetosphere than one at *Io*'s orbit.

Correlation studies of Terasawa *et al.*³⁶, Oya and Morioka¹⁶¹ and recently by Bose and Bhattacharya^{47,48} supported the fact that *Io*-independent DAM is very much dependent on different solar parameters and which is also supported by Galileo spacecraft data¹⁵. Further evidence of this interaction is now available in *in-situ* detection of a propagating Alfvén wave close to the *Io* flux tube, the infrared (IR) and the ultraviolet (UV) imaging of the ionospheric emission at the foot of the *Io* flux tube (Figs 5 and 6). Unlike the terrestrial aurora, the Jovian aurora is thought to come from two sources, field aligned currents (FAC's) from the moon *Io*, and from currents carrying particles from somewhere deeper in Jupiter's magnetotail. The streams of particles responsible for the aurora are thought to generate a type of radio emission called DAM. On Earth, Hiss is thought to occur when particles are being forced into the auroral zone. Jupiter's magnetosphere is far different from the Earth's, so scientists studying the aurora of Jupiter look for DAM and other radio signals as proof of how the aurora is generated.

These observation are interpreted in the frame of two models, the "Unipolar inductor model" (Fig. 24) proposed by Goldreich and Lynden Bell³¹ after DAM modulation discovery and the "Open loop Alfvén wave model" (Fig. 25) proposed by Neuber⁵⁵ and Goertz¹⁶² based on the detection of the magnetic perturbation and plasma density perturbation by Voyager 1 close to the *Io* flux tube. These two models actually represent two versions of the same interaction between *Io* and the magnetized torus but non-explicitly include a process that accelerates particles

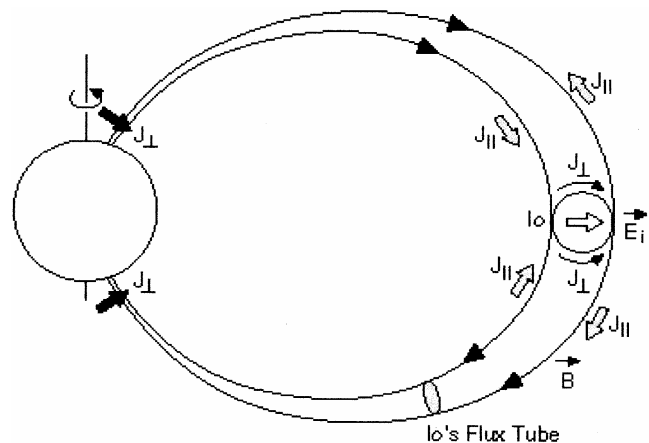


Fig. 24 — The classical unipolar inductor model to explain *Io*-controlled radio emission from Jupiter [Piddington and Drake, 1968; and Goldreich and Lynden-Bell, 1969]

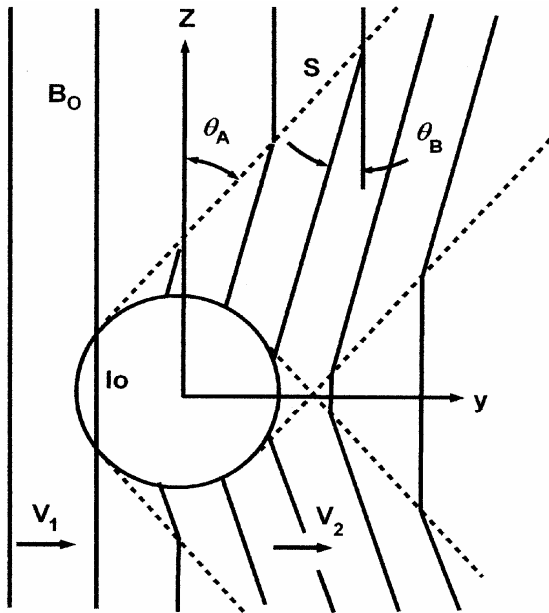


Fig. 25 — The open-loop Alfvén wave model. Sketch of the magnetic field distortion caused by Alfvén waves that are generated by the *Io*/torus interaction [The waves propagate along the Jovian magnetic field B_0 in the plasma reference frame. These Alfvén waves form an Alfvén wing whose local angle θ_A to the Jovian magnetic field varies with the local plasma condition (from Hill *et al.*, 1983).]

along the field lines. The relative motion of *Io* in the co-rotating plasma torus disturbs the magnetic field of Jupiter. The propagation of the perturbation away from *Io* is usually described as a propagation of low frequency magneto hydrodynamic (MHD) waves. Most of the energy will propagate along the *Io* flux tube as Alfvén waves. The magnetic perturbation induces a field-aligned current that propagates down towards the Jovian ionosphere along the *Io* flux tube. Basic difference of the two models is the location of the field-aligned current closure. In the unipolar inductor model, the current closes in the Jovian ionosphere as a Pedersen current, while in the open loop Alfvén wave model, the current closes at the front of the Alfvén wave as polarization current. Both the models are required to explain different features of emissions from Jovian magnetosphere. On one hand, the observation of *Io*- related DAM emission usually favours the unipolar inductor model as it is able to provide a large lead - angle (the ionospheric foot of the Alfvén wing leads *Io* by an angle called the lead angle) close to 15° that would explain the observed asymmetry in radio emissions on the other hand, the open loop Alfvén wave model can explain the DAM spectra show a "multiple - arc" modulation pattern (arcs in a time-frequency diagram), which are

usually interpreted as multiple bounces of standing Alfvén waves trapped between the torus and the Jovian ionosphere^{63,70}. Far-field effects of the *Io*-Jupiter interaction include acceleration and precipitation of electrons into Jupiter's ionosphere leading to UV, IR and radio emissions at/near the *Io* Flux Tube (IFT) footprints¹⁶³.

Remote observations are well adapted to study these electromagnetic signatures; whose existence demonstrates that *Io*'s influence extends down to Jupiter's ionosphere. They are complementary to *in-situ* observations close to *Io*. Besides these observations (IFT footprints and observations close to *Io*), nothing is known about the disturbance induced by *Io* except for some indirect information from radio emission. Galileo, Hubble Space Telescope (HST) and Cassini observations had shown similar but less energetic effects to occur at the footprints of the other Galilean satellites¹⁶⁴. Studying right handed polarized *Io*-DAM arcs from the northern hemisphere, Queinsec and Zarka²⁵ observed radio fringes with ~ 2 min spacing preceding the main arc (Fig. 26), and explained the phenomenon by multiple reflections of the Alfvén wave perturbation between Jupiter's ionosphere and the external boundary of the torus^{52,59} for which they could estimate a reflection coefficient of $\sim 95\%$. Their counterpart of the faint extended in UV and IR trails of spots separated by 1° to 2° detected downstream of *Io*'s foot prints, and which could be interpreted in terms of wave reflections¹⁶⁵; wake reacceleration¹⁶⁶. Connerney and Satoh¹⁶⁷ observed multiple features at the foot of the *Io* flux tube in imagery with approximately 4-5 deg separation between subsequent spots. Multiple features were infrequently observed, but on several occasions a pair of emission features had been observed in both H_3^+ imagery¹⁶⁷ and in the UV¹⁶⁸.

Queinsec and Zarka²⁵ also proposed an alternative scenario for the weak radio arc following the main arc [Fig. 26 (a),(c)], in which accelerated electrons leak from the Alfvénic perturbation on their way to Jupiter, and produce – after mirroring – low intensity radio emission in a narrow band just below the maximum surface gyrofrequency. Combining ground-based Nancay observatory data and WIND -WAVES spacecraft observations, *Io*-DAM arcs can be observed from ~ 40 MHz down to ~ 1 -2 MHz [Fig. 26(a)], i.e. from just above the ionosphere to $1 - 2R_J$ above it. The low-frequency cut-off in the dynamic spectra of DAM arcs is seen to lie between 1 and 2 MHz, whereas the minimum electron gyro

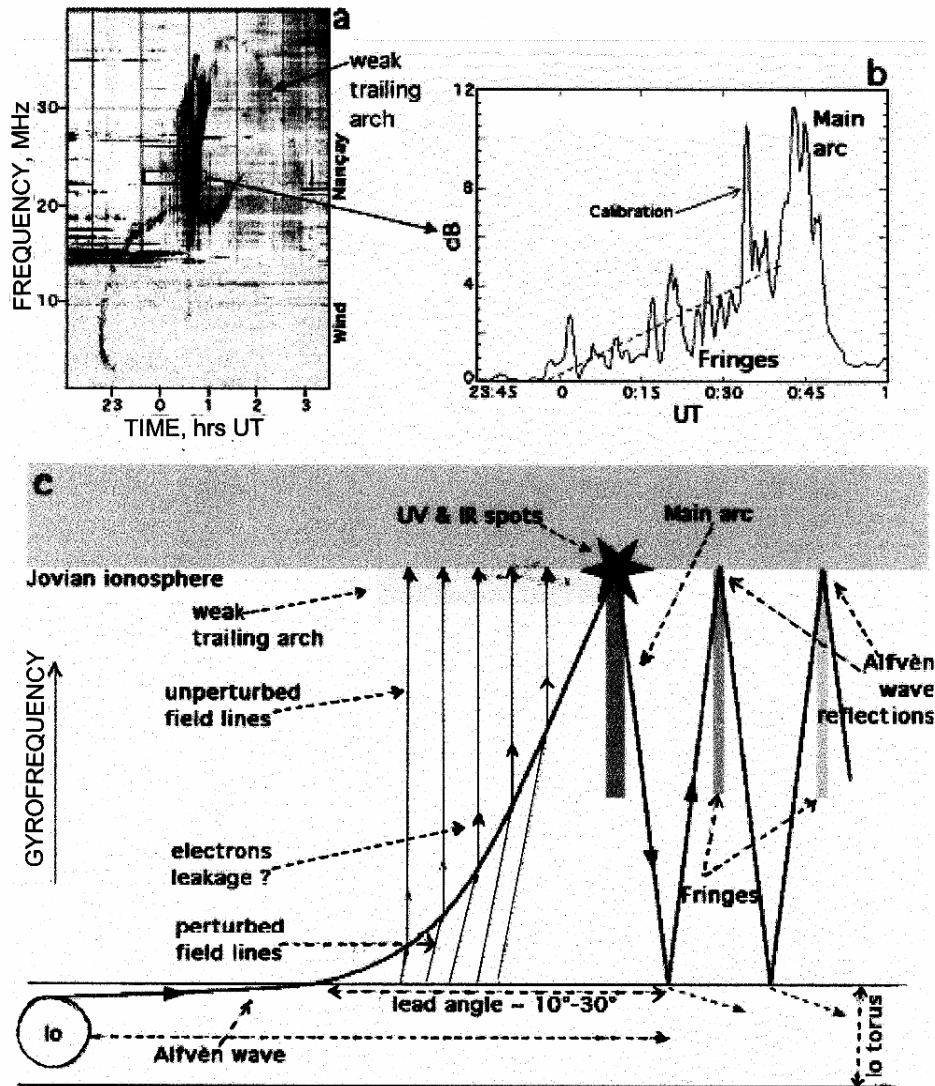


Fig. 26 — (a) Alfvén wave perturbation between Jovian ionosphere and the external boundary of the *Io* torus and corresponding features-*Io*-DAM dynamic spectrum arcs, (b) intensity distribution over 1 MHz band at 23 MHz, showing the main arc preceded by fringes with ~ 2 min spacing (--- indicates intensity ratio from one fringe to the next); *Io*-Jupiter interaction deduced from (a) and (b) [*---- represents most of the energy is deposited at the first arrival of the perturbation to the ionosphere. Adapted from Zarka *et al.*, 1998]

frequency is ~ 60 kHz. Zarka *et al.*¹⁶⁹ proposed that *Io*-DAM is produced along field lines threading through the dense, stagnating plasma wake discovered by Galileo¹⁷⁰; the vertical extent of the wake can then lead to quenching of the cyclotron-Maser mechanism below 1-2 MHz, provided that it contains protons with a concentration > 1 -3%. Using the O6 and VIP4 field models, Zarka²⁸ proposed 3D modelling over the full 1-40 MHz frequency range [Fig. 26(a)] and showed that the arc shape appeared in the dynamic spectra of Jovian DAM is quantitatively consistent with the emission coming from a single flux tube fixed in *Io*'s frame, leading *Io* by $\sim 10^\circ$ - 30° . The detailed arc shape can be obtained from the combination of nonplanar

field line topology with radio emission beaming in a conical sheet of $70^\circ \pm 5^\circ$ aperture (half-angle) and $\sim 2^\circ$ thickness¹⁷. The Jovian radio emission-beaming angle must slightly decrease with increasing frequency²⁴ and also it is observed that the arc shape can vary with the beaming angle.

All the above theoretical and experimental discussions have been based on the strong control of the DAM emissions by the satellite *Io* through standing Alfvén waves^{56,171}. Erkaev *et al.*¹⁷² tried to draw attention to the less intensive slow mode magnetohydrodynamic (MHD) waves, which received less attention on such interaction. Though in different publications^{173,174}, these types of waves were

investigated to the vicinity of *Io*, none proceeded further to investigate the consequences of propagation of such waves into the strong magnetic field region above the ionosphere. Erkaev *et al.*¹⁷² using the experimental data of the plasma pressure (Fig. 27) in the vicinity ($\sim 0.5R_{Io}$), i.e. 900 km of *Io* provided by the Galileo space craft¹⁷⁵ and extrapolating the trend of the curve with a Gaussian function predicted that the real enhancement of the gas pressure must be in the range $6-8R_J$ in the warm plasma of the torus around *Io* and estimated the consequences of the slow wave propagation processes along the *Io*-flux tube ($L \sim 6$) due to such enhancement. During its orbital

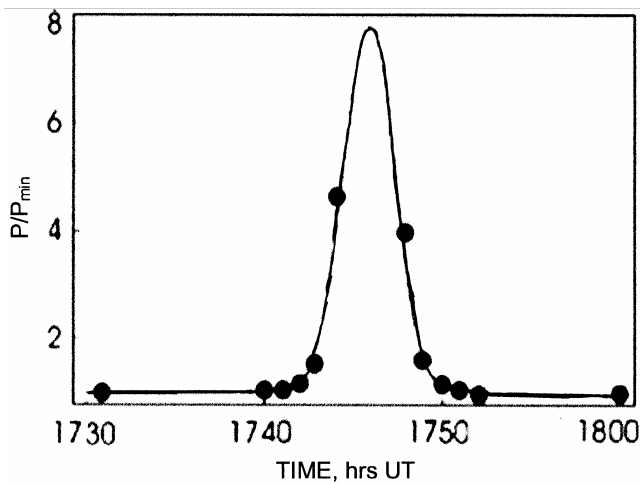


Fig. 27 — Extrapolation of the plasma pressure with Gaussian functions [Data points obtained by the Galileo spacecraft. Adapted from Erkaev *et al.*, 2002.]

motion *Io* is followed by a wake of disturbed plasma pressure. In the reference frame fixed to *Io*, these wings look like a steady structure. However, in a frame of a given magnetic flux passed by *Io*, the plasma perturbations are not steady i.e. the plasma pressure is a function of time. They assumed also that the relaxation time of attaining equilibrium of the background plasma parameters of the magnetic flux tube should be much less than the period of *Io*-motion along its orbit as well as for the *Io*-Jupiter interaction. From the physical point of view as slow mode wave is guided along the magnetic field and propagates inside a dipole flux tube with progressively decreasing cross-section (within a distance of $7.13R_J$ the cross-section decreases by 380 times) the magnetic pressure increases by 1.5×10^5 times. As a consequence, the flow velocity has to increase toward Jupiter rather than to decrease as it is usually observed after a regular explosion phenomenon.

With such physical picture Erkaev *et al.*¹⁷² described the slow mode wave mechanism (Fig. 28) as a pressure pulse produced near *Io* generates two slow MHD waves propagating along the IFT in the opposite directions – one towards the northern and the other towards the southern ionosphere of Jupiter. These slow mode MHD waves are quickly converted by steepening mechanism due to supersonic flow behind the shock front into non-linear waves. The velocity of the wave behind the shock increases in its course of propagation to Jupiter and attains the values of the order of the initial Alfvénic velocity (~ 150 km

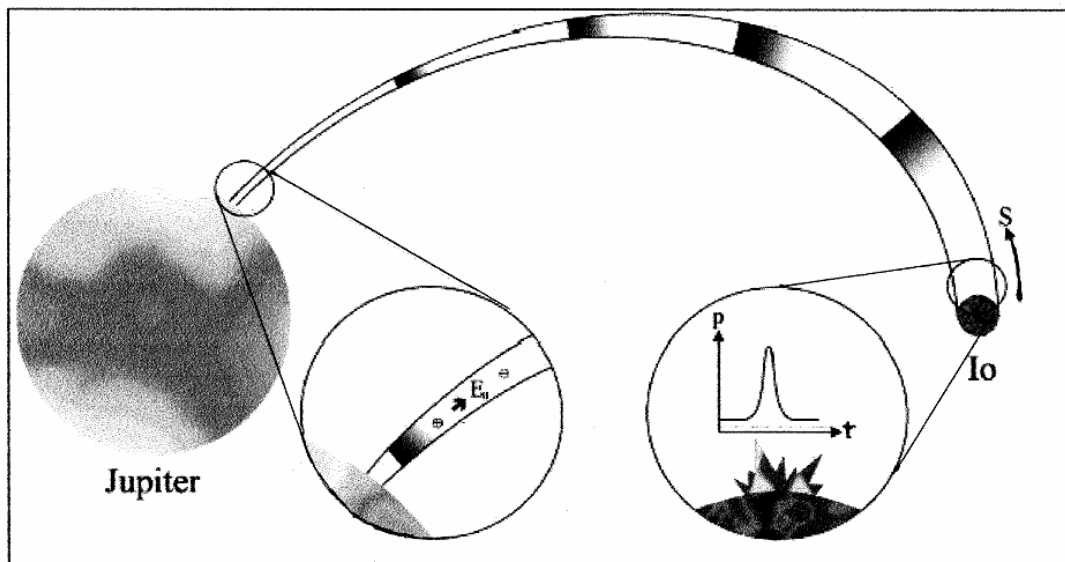


Fig. 28 — Schematic view of the development of a non-linear slow-mode wave and a field aligned electric field due to pressure pulse at *Io* [Parameter S represents the distance measured along *Io*-flux tube. Adapted from Erkaev *et al.*, 2002.]

s^{-1}) near I_o . As a consequence the plasma flow streaming along the I_o flux tube has to generate a field aligned potential difference (~ 1 kV) due to the Alfvén mechanism. By this way slow mode wave mechanism as proposed by Erkaev *et al.*¹⁷² can take a competitive part to explain the phenomena like I_o -controlled aurora and radio emissions together with the generally accepted Alfvén wings model.

Though the arrival of Alfvén wave at the Jovian ionosphere take the leading role of explaining the existing phenomena, e.g. trailing spots as mentioned earlier have been interpreted as arrivals of reflected Alfvén waves¹⁷⁶. Erkaev *et al.*¹⁷² claimed that one of such bright spots in the tail might be connected with the arrival of the slow shock. Queinnec and Zarka²⁵ pointed out that the maximum emission frequency of some parts of the DAM emission, in particular the I_o -B radiation; require a 30° - 50° lag of the source field line and the instantaneous I_o flux tube. The propagation time of Alfvén waves considering this lag would require unrealistically increasing plasma density (more than 10 times higher than that used by Bagenal¹⁷⁷). But, this can be estimated without considering such inflated plasma density with the Erkaev *et al.*¹⁷² model. According to them the consequence of the slow shock propagation is a strong plasma flow behind the shock front, which in turn leads to a field-aligned potential difference of the order of 1 kV. The said 30° - 50° lag in longitude can easily be interpreted, as the non-linear wave is much slower than an Alfvén wave. Under such consideration they claimed the slow wave mechanism could be considered as responsible for some parts of the DAM emissions.

6 Scope for further investigation

Regarding the DAM dynamic spectral arcs one can draw some conclusions, which are more definite and less model dependent. Convincing evidences reveal that the observed I_o -A and I_o -C principal arc emission originates in the vicinity of the northern foot of the instantaneous I_o flux tube, on the basis of the hollow cone-beaming hypothesis. The estimated cone half-angle decreases with increasing frequency above the noise frequency in each case, which is consistent with the cone half-angle variation proposed by Goldstein and Thieman⁶⁷ at every frequency the cone half-angle determined for Voyager 2 was greater than that for Voyager 1. This is, in fact, evidence of greater refraction of those rays leaving the source that are destined for the lower declination spacecraft than for those that will reach the higher declination one.

Observations of the sense of elliptical polarization of the two emission events have been considered in the light of the cyclotron maser emission mechanism. The dominant polarization sense of the principal arc emission in both cases was consistent with that of R-X mode radiation from the northern foot of the I_o flux tube. Such principal arc emission is perhaps caused by electron with energies greater than about 2 keV on the basis of the theoretical results of Wong *et al.*¹⁷⁸ There appears to be a number of groups of secondary arcs associated with each principal arc. All of the emission in the two events investigated in the form of both secondary and primary arcs, originated in the northern hemisphere but that the LH polarization of the I_o -C secondary arcs at the lower frequencies was emitted in the ordinary mode by relatively low energy electrons. The so called splitting¹³⁵ structure of Jovian DAM dynamic spectra which manifests itself as one or several bands of emission “detached” in the f - t plane from the main DAM emission is still unexplained. If this result can be verified, it will be of considerable importance for developing the theory of the Jovian decametric emission mechanism. The so called splitting¹³⁵ structure of Jovian DAM dynamic spectra which manifests itself as one or several bands of emission “detached” in the f - t plane from the main DAM emission is still unexplained.

There are some major consequences owing to the field-aligned currents to the middle magnetosphere and the associated electrical connections of the ionosphere. The scenario has importance for answering a number of questions raised by the Voyager observations. They are related to extensive local plasma heating, high-energy tails of protons, ion, and relative electron^{176,177} and high power electron bombardment of the atmosphere and also on energetic proton deposition from the ionosphere to the magnetosphere. A detailed examination of the available data should depict the degree to which these mechanisms are operating at Jupiter.

Searching for DAM occultations of IFT by the satellite Ganymede Arkhipov¹⁸⁰ found that the ratio of the emitted frequency of I_o -A source to the calculated gyromagnetic frequency of electrons in the source is 1.11 ± 0.02 . Formally this theory contradicts the present CMI theory, the requirement of which is that f_c should be very much closure to 1 and this non-agreement needs the improvement of the magnetic field model or the basic mechanism.

As it has already been known to us from terrestrial as well as different spacecraft observations that solar

wind exerts a notable influence on broad band kilometric (bKOM), Hectometric (HOM), and non-*Io* DAM through its magnetic sector structure^{28,48,161} and density fluctuations, and a much weaker one, if any, on the *Io*-DAM¹⁸¹⁻¹⁸⁴. This has been considered as belonging to the high latitude of the former radio sources, while the inner Jovian magnetosphere and, consequently the *Io*-DAM, produced in the IFT vicinity along $L = 6$ field lines, was thought to be protected from external conditions by closed Jovian magnetic field lines. But a significant influence of the solar wind has also been found on the occurrence of kilometric (nKOM) component, for which sources are embedded in the *Io*-plasma torus¹⁶¹. It is thus important to check the existence and degree of solar wind control of *Io*-DAM in order to then address the question of its generation in the inner magnetosphere.

One of the major unresolved questions involves *Io*'s far-field plasma interaction. How does the coupling mechanism between *Io* and Jupiter's ionosphere function occur?

There is a lacuna in our knowledge about the magnetospheric properties such as plasma densities and electron and ion temperatures at higher latitudes.

The mechanism that accelerates the electrons necessary to excite *Io*'s footprint is also not known.

The origin of the bi-directional electron beams in the wake of *Io* is not understood.

Other transport processes along the field lines, such as mass transport, i.e. via slow-mode waves have not been studied in enough details.

Mass loading at *Io* is also a subject that deserves more attention. The canonical value for the total mass rate is 1 ton-s^{-1} (Broadfoot *et al.*¹⁷⁶), derived from Voyager observations 185. This number might undergo temporal variations and should be confirmed by further analysis. It is currently not clear how this mass rate is supplied to *Io*'s torus. Most mass leaves *Io* as neutrals. Shemansky¹⁸⁶ and Bagenal¹⁸⁷ estimated that only 20-50% is locally ionized at *Io*, while Saur *et al.*¹⁸⁸ reduced the limit to $< 20\%$. An important mechanism for the neutral mass loss could be sputtering by torus ions^{189,190}. Modeling of the sputtering is a difficult task, since the region around *Io*'s exosphere needs to be treated appropriately. Neither collision-free models nor fluid models can be applied. A model of *Io*'s multi-ion chemistry that self-consistently includes the plasma physics in three dimensions has not yet been undertaken and will lead to important new results. The current models are at one extreme self-consistent 3D one-fluid MHD

models^{191,192}. The models by Saur *et al.*^{193,194} are partly self-consistent, 3D, and two-fluid, where the electrons energetics are treated accurately. The feedback mechanisms of *Io*'s atmosphere and the plasma interaction too is relatively poorly understood. The plasma interaction modifies the general structure¹⁹⁴ as well as the temperature of the atmosphere¹⁹⁵, while in turn a modified neutral atmosphere will affect the plasma interaction.

Acknowledgements

The authors are grateful to their respective Heads for their encouragement and providing facilities. Authors are extremely grateful to the Reviewer of this paper for his highly valuable comments and suggestion. In fact, the paper has got its present form only because of his careful review and very important suggestions throughout for improving the paper.

References

- 1 Burke B F & Franklin K L, Observations of variable radio source associated with the planet Jupiter, *J Geophys Res (USA)*, 60 (1955) 213.
- 2 Thieman J R, A catalog of Jovian decametric radio observations from 1957 – 1978, *NASA Technical Memorandum*, 1979, 8308.
- 3 Kaiser M L, A Low-Frequency Survey of the Planets with RAE, *J Geophys Res (USA)*, 82 (1977) 1256.
- 4 Bougeret J L, Kaiser M L, Kellog P, Manning R, Goertz K, *et al.*, The Wind/ WAVES instrument, *Space Sci Rev (USA)*, 71 (1995) 231.
- 5 Smith E J, Davis L Jr., Jones D E, Coleman P J & Colburn D S, The planetary magnetic field and magnetosphere of Jupiter: Pioneer10, *J Geophys Res (USA)*, 279 (1974) 3501.
- 6 Smith E J, Davis L Jr., Jones D E, Coleman P J & Dyal P, Jupiter's magnetic field, magnetosphere, and interaction with the solar wind: Pioneer 11, *Science (USA)*, 188 (1975) 451.
- 7 Acuna M H & Ness N F, Results from the GSFC fluxgate magnetometer on Pioneer 11, *Jupiter*, Edited by T Gehrels (University of Arizona Press, Tucson, Arizona), 1976, p.830.
- 8 Acuna M H & Ness N F, The main magnetic field of Jupiter, *J Geophys Res (USA)*, 81 (1976) 2917.
- 9 Warwick J W, Pearce J B, Riddle A C, Alexander J K, Desch M D, Kaiser M L, Thieman J R, Carr T D, Gulkis S, Boischoat A, Harvey C C & Pederson B M, Voyager 1 planetary radio astronomy observations near Jupiter, *Science (USA)*, 204 (1979a) 995.
- 10 Warwick J W, Pearce J B, Riddle A C, Alexander J K, Desch M D, Kaiser M L, Thieman J R, Carr T D, Boischoat A, Leblanc Y, Pederson B M & Staelin D H, Planetary radio astronomy observations from Voyager 2 near Jupiter, *Science (USA)*, 206 (1979b) 991.
- 11 Alexander J K & Carr T D, Synoptic observations of Jupiter's radio emissions – Average statistical properties observed by Voyager, *J Geophys Res (USA)*, 86 (1981) 8529.
- 12 Gurnett D A, Kurth W S, Shaw R R, Roux A, Gerding R, Kennel C F, Scarf F L & Shawhan S D, The Galileo plasma wave investigation, *Space Sci Rev (USA)*, 60 (1992) 341.

- 13 Gurnett D A, Kurth W S, Ronix A, Bolton S J & Kennel C F, Galileo plasma wave observations in the Io plasma torus and near Io, *Science (USA)*, 274 (1996) 391.
- 14 Meniotti J D, Gurnett D A, Kurth W S, Groene G B & Granroth L J, Radio emissions observed by Galileo near Io, *Geophys Res Lett (USA)*, 25 (1998a) 25.
- 15 Meniotti J D, Gurnett D A, Kurth W S, Groene G B & Granroth L J, Galileo direction finding of Jovian radio emissions, *J Geophys Res (USA)*, 103 (1998b) 20001.
- 16 Barrow C H, Huang S, Macdowall R J & Lecacheux A, Kilometre-wave radio observations of solar type III bursts by Ulysses compared with decametre-wave observations from the Earth, *Astron Astrophys (Germany)*, 316 (1996) 413.
- 17 Kaiser M L, Zarka P, Kurth W S, Hospodarsky G B & Gurnett D A, Cassini and Wind stereoscopic observations of jovian non-thermal radio emissions: measurements of beam widths, *J Geophys Res (USA)*, 105, A7 (2000) 16053.
- 18 Klecker K M, Higgins C A & Meniotti J D, *Satellite Influence on Jupiter's Radio Emission*, American Astronomical Society Meeting 202, # 33.01, 2003.
- 19 Bigg E K, Influence of the satellite Io on Jupiter's decametric emission, *Nature (UK)*, 203 (1964) 1008.
- 20 Kaiser M L & Alexander J K, Terrestrial Kilometric Radiation: 3-Average Spectral Properties, *J Geophys Res (USA)*, 82 (1977) 3273.
- 21 Carr T D, Desch M D & Alexander J K, *Phenomenology of magnetospheric radio emissions, Physics of the Jovian Magnetosphere*, Edited by A J Dessler (Cambridge Univ. Press, Cambridge, NY), 1983, pp.226-284.
- 22 Dulk G A, Io-related radio emission from Jupiter, *Icarus (USA)*, 7 (1967) 173.
- 23 Boischot A, Lecacheux A, Kaiser M L, Desch M D, Alexander J K & Warwick J W, Radio Jupiter after Voyager: An overview of the Planetary Radio Astronomy Observations, *J Geophys Res (USA)*, 86 (1981) 8213.
- 24 Lecacheux A, Boudjada M Y, Rucker H O, Bougeret J L, Manning R & Kaiser M L, Jovian decameter emissions observed by the Wind Waves radioastronomy experiment, *Astron Astrophys (Germany)*, 329 (1998) 776.
- 25 Queinnee J & Zarka P, Io-controlled decameter arcs and Io-Jupiter interaction, *J Geophys Res (USA)*, 103 (1998) 26649.
- 26 Aubier A, Boudjada M Y, Moreau P H, Galopeau P H M, Lecacheux A & Rucker H O, Statistical studies of jovian decameter emissions observed during the same period by Nancy Decameter Array (France) and WAVES experiment aboard Wind spacecraft, *Astron Astrophys (Germany)*, 354 (2000) 1101.
- 27 Wu C S & Lee L C, A theory of the terrestrial kilometric radiation, *Appl Phys J (UK)*, 230 (1979) 621.
- 28 Zarka P, Auroral radio emissions at the outer planets: observations and theories, *J Geophys Res (USA)*, 103 (1998) 20159.
- 29 Piddington J H & Drake J F, Electrodynamical effects of Jupiter's satellite Io, *Nature (UK)*, 217 (1968) 935.
- 30 Willes A J, Melrose D B & Robinson P A, Elliptically polarized Jovian decametric radiation: an investigation of the electron cyclotron maser mechanism, *J Geophys Res (USA)*, 99 (1994) 21203.
- 31 Goldreich P & Lynden Bell B, Io, a Jovian unipolar inductor, *Astrophys J (UK)*, 156 (1969) 59.
- 32 Neubauer F M, Nonlinear standing Alfvén wave current system at Io: Theory, *J Geophys Res (USA)*, 85 (1980) 1171.
- 33 Hill T W, Dessler A J & Goertz C K, Magnetospheric models, *Physics of the Jovian Magnetosphere*, Edited by A J Dessler (Cambridge Univ. Press, Cambridge, NY), 1983, pp.353-394.
- 34 Pontius Jr. D H, The Io current wing, *J Geophys Res (USA)*, 107 (2002) 1.
- 35 Barrow C H, Jupiter's decametric emission and solar activity, *Planet Space Sci (UK)*, 26 (1978) 1193.
- 36 Terasawa T, Maezawa K & Machida S, Solar wind effect on Jupiter's non-Io-related radio emission, *Nature (UK)*, 273 (1978) 131.
- 37 Levitskij L S & Vladimiskij B M, The effect of interplanetary magnetic field sector structure on the decametric wave emission of Jupiter, *Izv Krym Astrofiz Obs (Russia)*, 59 (1979) 104.
- 38 Barrow C H, Association of corotating magnetic sector structure with Jupiter's decameter-wave radio emission, *J Geophys Res (USA)*, 84 (1979) 5366.
- 39 Barrow C H, Latitudinal Beaming and local time Effects in the decameter-wave Radiation from Jupiter observed at the Earth and from Voyager, *Astron Astrophys (Germany)*, 101 (1981) 142.
- 40 Pokorney Z, Decametric emission of Jupiter and solar activity, *Bull Astron Inst (Czechoslovakia)*, 33 (1982) 193.
- 41 Penkulu E R, Influence of interplanetary magnetic field sector boundary passages on Jovian decametric radio bursts, *Planet Space Sci (UK)*, 31 (1983) 129.
- 42 Bose S K, Mitra B & Ganguly S R, The change of Jovian decametric radio emission during an apparition, *National Space Science Symposium Proceedings*, 1983, 212.
- 43 Bose S K, Mitra B, Ganguly S R & Sastri R C, Influence of Solar Wind streams on non-Io related decametric emission of Jupiter, *Indian J Radio Space Phys*, 14 (1985) 50.
- 44 Woch J, Krupp N, Lagg A, Wilken B & Livi S, Quasi-periodic modulations of the Jovian magnetotail, *Geophys Res Lett (USA)*, 25 (1998) 1253.
- 45 Bose S K & Bhattacharya A B, On some aspects of non-Io Decametric emission from Jupiter and solar plasma, *XI National Space Science Symposium Proceedings*, 2000, 257.
- 46 Bose S K & Bhattacharya A B, Local time dependence of decametric radio emission from Jupiter observed from Earth stations at different Solar activity, *Indian J Radio Space Phys*, 30 (2001) 232.
- 47 Bose S K & Bhattacharya A B, Comparison of ground based observations with spacecraft observations of decametric radio emission from Jupiter, *National Space Science Symposium Proceedings*, 2002, 354.
- 48 Bose S K & Bhattacharya A B, Solar plasma activated DAM of non-Io origin from Jupiter magnetosphere, *Indian J Radio Space Phys*, 32 (2003) 43.
- 49 Gurnett D A, Kurth W S, Hospodarsky G B, Pederson A M, Zarka P, Lecacheux A, Bolton S J, Desch M D, Farrells W M, Kaiser M L, Ladreiter H P, Rucker H O, Galopeau P, Louren P, Young D T, Pryor W R & Dougherty M K, Control of Jupiter's radio emission and aurora by the solar wind, *Nature (UK)*, 415 (2002) 985.
- 50 Meniotti J D, Gurnett D A, Kurth W S & Groene J B, Local time dependence of Jovian radio emissions observed by Galileo, *Geophys Res Lett (USA)*, 26 (1999) 569.
- 51 Morioka A, Tsuchiya F, Miyoshi Y, Misawa H, Oya H & Furukawa K, Duration of Jovian magnetospheric disturbances inferred from decametric radio storms, *Earth Planets Space (UK)*, 54 (2002) 1277.

- 52 Gurnett D A & Goertz C K, Multiple Alfvén wave reflections excited by Io Origin of the Jovian decametric arcs, *J Geophys Res (USA)*, 86 (1981) 717.
- 53 Bagenal F, Alfvén wave propagation in the Io plasma torus, *J Geophys Res (USA)*, 88 (1983) 3013.
- 54 Bagenal F & Sullivan J D, Direct plasma measurements in the Io torus and inner magnetosphere of Jupiter, *J Geophys Res (USA)*, 86 (1981) 8447.
- 55 Smith P R & Wright A N, Multiscale periodic structure in the Io wake, *Nature (UK)*, 339 (1989) 452.
- 56 Neubauer F M, Nonlinear standing Alfvén wave current system at Io, *J Geophys Res (USA)*, 85 (1980) 1171.
- 57 Wright A N & Smith P R, Periodic features in the Alfvén wave wake of Io, *J Geophys Res (USA)*, 95 (1990) 3745.
- 58 Staelin D H, Garnavich P M & Leblanc Y, Jovian decametric arcs and Alfvén currents, *J Geophys Res (USA)*, 93 (1988) 3942.
- 59 Bagenal F & Leblanc Y, Io's Alfvén wave pattern and the Jovian decametric arcs, *Astron Astrophys (Germany)*, 197 (1988) 311.
- 60 Belcher J W, Lazarus A J, Sullivan J D, McNutt R L, Bagenal F, Scudder J D, Sitter E C, Siscoe G L, Vasyliunas V M, Goertz C K & Yeates C M, Plasma observations near Jupiter: Initial results from Voyager 1, *Science (USA)*, 204 (1979) 987.
- 61 Bagenal F, Empirical model of the Io plasma torus: Voyager measurements, *J Geophys Res (USA)*, 99 (1994) 11043.
- 62 Frank L A, Paterson W R, Ackerson K L, Vasyliunas V M, Coroniti F V & Bolton S J, *Science (USA)*, 204 (1979) 972.
- 63 Prang R, Rego D, Southwood D, Zarka P, Miller S & Ip W H, Rapid energy dissipation and variability of the Io-Jupiter electrodynamic circuit, *Nature (UK)*, 379 (1996) 323.
- 64 Wilkinson M H, Co-related jovian decametric arcs, *J Geophys Res (USA)*, 94 (1989) 11777.
- 65 Maeda K & Carr T D, Measurement of Jovian decametric Io related source location and beam shape, *J Geophys Res (USA)*, 97 (1992) 1549.
- 66 Riddle A C, Identification of radio emission from Io flux tube, *J Geophys Res (USA)*, 88 (1983) 455.
- 67 Goldstein M L & Thieman J R, The formation of arcs in the dynamic spectra of Jovian decameter bursts, *J Geophys Res (USA)*, 86 (1981) 8569.
- 68 Wilkinson M H, Evidence for periodic modulation of Jupiter's decametric radio emission, *J Geophys Res (USA)*, 103 (1998) 19985.
- 69 Leblanc Y, On the arc structure of the DAM Jupiter emissions, *J Geophys Res (USA)*, 86 (1981) 8546.
- 70 Cray F J & Bagenal F, Coupling the plasma interaction at Io to Jupiter, *Geophys Res Lett (USA)*, 24 (1997) 2135.
- 71 Connerney J E P, Baron R, Satoh T & Owen T, Images of excited H⁺ at the foot of the Io flux tube in Jupiter's atmosphere, *Science (USA)*, 262 (1993) 1035.
- 72 Zarka P, Ryabov B P, Ryabov V B, Prange' R, Abda Simon M, Farges T & Denis L, On the origin of Jovian decameter radio bursts, IV, *Planetary Radio Emissions*, Edited by H O Rucker, S J Bauer and A Lecacheux, (Austrian Acad. Sci. Press, Vienna), 1997, p.51.
- 73 Lecacheux A, Meyer-Vernet N & Daigne G, Jupiter's decametric radio emission; A nice problem of optics, *Astron Astrophys (Germany)*, 94 (1981) L-9.
- 74 Calvert W, A feedback model for the source of auroral kilometric radiation, *J Geophys Res (USA)*, 87 (1982) 8199.
- 75 Lecacheux A, Boisshot A, Boudjada M Y & Dulk G A, Spectra and complete polarization state of two, Io related, radio storms from Jupiter, *Astron Astrophys (Germany)*, 251 (1991) 339.
- 76 Leblanc Y, Dulk G A & Bagenal F, On Io's excitation and the origin of Jupiter's decametric radiation. *Astron Astrophys (Germany)*, 290 (1994) 660.
- 77 Dulk G A, Leblanc Y & Lecacheux A, The complete polarization state of Io-related radio storms from Jupiter: A statistical study Astronomy and Astrophysics, *Astron Astrophys (Germany)*, 286 (1994) 683.
- 78 Genova F, Zarka P & Barrow C H, Voyager and Nancay observations of the Jovian radio-emission at different frequencies – Solar wind effect and source extent, *Astron Astrophys (Germany)*, 182 (1987) 159.
- 79 Stone R G, Bougeret J L, Caldwell J, Canu P, DeConchy Y, Cornilleau-Wehrin N, Desch M D, Fainberg J, Goetz K, Goldstein M L, Harvey C C, Hoang S, Howard R, Kaiser M L, Kellogg P J, Klein B, Knoll R, Lecacheux A, Lengyel-Frey D, R. MacDowall J, Manning R, Meetre C A, Meyer A, Monge N, Monson S, Nicol G, Reiner M J, Steinberg J L, Torres E, deVilledary C, Wouters F & Zarka P, The Unified Radio and Plasma Wave Investigation., *Astron Astrophys Suppl Ser (Germany)*, 92 (1992) 291.
- 80 Ladreiter H P & Leblanc Y, The Jovian hectometric radiation: An overview after the Voyager mission, *Ann Geophys (France)*, 9 (1991) 784.
- 81 Boisshot A, Sastri J H & Zarka P, Localization of Io and non-Io sources of Jovian decameter emission, *Astron Astrophys Suppl (UK)*, 175 (1987) 287.
- 82 Kaiser M L & Garcia L N, Jupiter's Low Frequency Radio Spectrum: Filling in the Gaps, *Planetary Radio Emissions*, Edited by H O Rucker, S J Bauer and A Lecacheux, Vol.IV, (Austrian Acad Sci. Press, Vienna), 1997, p.17.
- 83 Genova F & Aubier M G, Io-dependent sources of the Jovian decameter emission, *Astron Astrophys (Germany)*, 150 (1985) 139.
- 84 Poquérusse M & Lecacheux A, First direct measurement of the beaming of Jupiter's decametric radiation, *Nature (UK)*, 275 (1978) 111.
- 85 Piddington J H, Electrodynamical effects of Jupiter's satellite Io, *Nature (UK)*, 217 (1968) 935.
- 86 Thieman J R & Smith A G, Detailed geometrical modeling of Jupiter's Io-related decametric radiation, *J Geophys Res (USA)*, 84 (1979) 2666.
- 87 Hashimoto K & Goldstein M L, A theory of the Io phase asymmetry of the Jovian decametric emission, *J Geophys Res (USA)*, 88 (1983) 2010.
- 88 Wang W X, An observationally compatible model for Jupiter's Io-related decametric emission, Ph D thesis, University of Florida, Gainesville, USA, 1985.
- 89 Pearce J B, A heuristic model for Jovian decametric arcs, *J Geophys Res (USA)*, 86 (1981) 8579.
- 90 Staelin D H, Character of the Jovian decametric arcs, *J Geophys Res (USA)*, 86 (1981) 8581.
- 91 Maeda K & Carr T D, Beam structure of Jupiter's decametric radiation, *Nature (UK)*, 308 (1984) 166.
- 92 Maeda K & Carr T D, Evidence for beaming of Jupiter's decametric radiation: Simultaneous observations from Voyagers and ground-based observatories, *Planetary Radio Emissions II*, Edited by H O Rucker, (Austrian Academy of Sciences, Vienna), 1988, p.95.

- 93 Genova F & Aubier M G, High frequency limit and visibility of the non-*Io* and *Io*-dependent Jovian decameter radio emission, *Astron Astrophys (Germany)*, 177 (1987) 303.
- 94 Aubier M G & Genova F, A catalogue of the high frequency limit of the Jovian decameter emission observed by Voyager, *Astron Astrophys Suppl (Germany)*, 61 (1985) 341.
- 95 Connerney J E P, Acunna M H & Ness N F, Modeling the jovian current sheet and inner magnetosphere, *J Geophys Res (USA)*, 86 (1981) 8370.
- 96 Desch M D, Farewell W M & Kaiser M L, Asymmetries in the *Io* plasma torus, *J Geophys Res (USA)*, 99 (1994) 17205.
- 97 Schneider N M, Taylor M H, Cray F J & Tranger J J, On the nature of the brightness asymmetry in the *Io* plasma torus, *J Geophys Res (USA)*, 102 (1997) 19823.
- 98 Thomas N & Lichtenberg G, The latitudinal dependence of ion temperature in the *Io* plasma torus, *Geophys Res Lett (USA)*, 24 (1997) 1175.
- 99 Goldstein M L & Goertz C K, Theories of radio emissions and plasma waves, *Physics of the Jovian Magnetosphere*, Edited by A J Dessler (Cambridge University Press, NY), 1983, p 317.
- 100 Green J L, The *Io* decametric emission cone, *Radio Sci (USA)*, 19 (1984) 2.
- 101 Leblanc Y, Bagenal F & Dulk G A, *Astron Astrophys (UK)*, 276 (1993) 603.
- 102 Smith R A, *Models of Jovian decametric radiation, Jupiter*, Edited by T Gehrels, (Univ. Arizona Press, Arizona, Tucson, USA), 1976, p.1146.
- 103 Zarka P, Cecconi B & Kurth W S, Jupiter's low frequency radio spectrum from Cassini/RPWS absolute flux density measurements, *J Geophys Res (USA)*, 109 (2004) 130.
- 104 Ellis G R A, The Jupiter radio bursts, *Proc Astron Soc Aust (Australia)*, 2 (1974) 1.
- 105 Riihimaa J J, S bursts in Jupiter's decametric radio spectra, *Astron Space Sci (USA)*, 51 (1977) 363.
- 106 Desch M D & Kaiser M L, Saturnian Kilometric Radiation: Satellite Modulation, *Nature (UK)*, 292 (1981) 739.
- 107 Leblanc Y, Genova F & de la Noe J, The Jovian S burst. I. Occurrence with L-bursts and frequency limit, *Astron Astrophys (Germany)*, 86 (1980) 342.
- 108 Riihimaa J J, Modulation Lanes in the Dynamic spectra of Jovian L bursts, *Astron Astrophys (Germany)*, 4 (1970) 180.
- 109 Genova F, Aubier M G & Lecacheux A, Modulations in jovian decametric spectra: Propagation effects in terrestrial ionosphere and Jovian environment, *Astron Astrophys (Germany)*, 104 (1981) 229.
- 110 Leblanc Y, Genova F & de la Noe J, *Astron Astrophys (Germany)*, 46 (1981) 135, 111.
- 111 Warwick J W, Dynamic spectra of Jupiter's decametric emission, 1961, *Astrophys J (USA)*, 137 (1963) 41.
- 112 Riihimaa J J, High-Resolution Spectral Observations of Jupiter's Decametric Radio Emission, *Nature (UK)*, 202 (1964) 476.
- 113 Warwick J W & Gordon M A, Frequency and Polarization Structure of Jupiter's decametric Emission on a 10-millisecond Scale, *Radio Sci (USA)*, 69 (1965) 1537.
- 114 Riihimaa J J, L-bursts in Jupiter's Decametric Radio Spectra, *Astrophys Space Sci (USA)*, 56 (1978) 503.
- 115 Douglas J N, Decametric radiation from Jupiter, *IEEE Trans Military Electron (USA)*, MIL-8 (1964) 173.
- 116 Douglas J N & Smith H, L-bursts in Jupiter's decametric radio spectra, *Astrophys J (UK)*, 148 (1967) 885.
- 117 Slee B & Higgins C S, The solar wind and Jovian decametric radio emission, *Aust J Phys (Australia)*, 21 (1968) 34.
- 118 Kraus J D, *Io* dependent Jovian radio emission, *Astron Astrophys (Germany)*, 53 (1976) 121.
- 119 Baart E E, Barrow C H & Lee R T, Millisecond radio pulses from Jupiter, *Nature (UK)*, 211 (1966) 808.
- 120 Barrow C H & Baart E E, B and C "sources" of Jovian decametric radiation, *Nature (UK)*, 213 (1967) 165.
- 121 Riihimaa J J, Evolution of the spectral Fine Structure of Jupiter's Decametric S-storms, *Earth, Moon and Planets (UK)*, 53 (1991) 157.
- 122 Boudjada M Y, Rucker H O, Ladreiter H P & Ryabov B P, Jovian S-bursts: the event of 4 January, *Astron Astrophys (Germany)*, 295 (1995a) 782.
- 123 Boudjada M Y, Rucker H O & Ladreiter H P, The *Io*-C Jovian decameter emissions, *Astron Astrophys (Germany)*, 303 (1995b) 255.
- 124 Boudjada M Y, Galopeau P H M, Rucker H O & Lecacheux A, Jovian narrow-band as generator of the Jovian millisecond radio bursts, *Astron Astrophys (Germany)*, 363 (2000) 316.
- 125 Riihimaa J J & Carr T D, Interactions of S- and L-bursts in Jupiter's decametric radio spectra, *Earth, Moon and Planets (UK)*, 25 (1981) 373.
- 126 Galopeau P H M, Boudjada M Y & Rucker H O, Drift of Jovian S-burst inferred from adiabatic motion in a parallel electric field, *Astron Astrophys (Germany)*, 341 (1999) 918.
- 127 Queinnee J & Zarka P, Flux, power, energy and polarization of Jovian S-bursts, *Planet Space Sci (USA)*, 49 (2001) 365.
- 128 Litvinenko G V, Vinogradov V V, Rucker H O, Leitner M & Shaposhnikov V E, Complex analysis of the Jovian S-bursts internal structure, *Geophys Res Abstr (UK)*, 5 (2003) 03772.
- 129 Litvinenko G V, Rucker H O, Vinogradov V V, Leitner M & Shaposhnikov V E, Internal structure of the Jovian simple S-burst obtained with the wavelet analysis technique *Astron Astrophys (Germany)*, 426 (2004) 343.
- 130 Litvinenko G V, Rucker H O, Taubenschuss U, Konovalenko A A & Lecacheux A, Dynamic spectrum features of the Jovian S-emission as obtained with different time scales, *Geophys Res Abstr (UK)*, 7 (2005) 02291.
- 131 Rucker H O, Taubenschuss U, Leitner M, Lecacheux A & Konovalenko A A, Superfine Structure of Jovian Millisecond Radio Bursts, *Am Geophys Union Joint Assn Suppl*, 17 (2004) 85.
- 132 Ergun R, *S-bursts and the Jupiter ionospheric Alfvén Resonator*, 6th International Workshop on Planetary and Solar Radio Emissions, Graz, Austria, 2005.
- 133 Riihimaa J J, Structured events in the dynamic spectra of Jupiter's decametric radiation, *Astron J (UK)*, 73 (1968) 265.
- 134 Boischoat A, Rosolen C, Aubier M G, Daigne G, Genova F, Leblanc Y, Lecacheux A, de la Noe J & Pedersen B M, A new high-gain broadband, steerable array to study Jovian decametric emissions, *Icarus (USA)*, 43 (1980) 399.
- 135 Leblanc Y & Rubio M, A narrow-band splitting at the Jovian decametric cutoff frequency, *Astron Astrophys (Germany)*, 111 (1982) 284.
- 136 Oya M, Oya H, Ono T & Iizima M, Analyses of Jovian Decametric Radiation S-bursts interacting with N-bursts, *Earth Moon Planets (Netherlands)*, 88 (2002) 187.
- 137 Arkhipov A V, On modulation lanes in spectra of the Jovian decametric radio emission: frequency drifts, *Kinematika Fiz Nebesnykh Tel (Ukraine)*, 19 (2003) 182.

- 138 Genova F & Leblanc Y, Interplanetary scintillation and Jovian Dam emission, *Astron Astrophys (Germany)*, 98 (1981) 133.
- 139 Lecacheux A, Meyer-Vernet N & Daigne G, Jupiter's decametric radio emission: A nice problem of optics, *Astron Astrophys (Germany)*, 94 (1981) L9.
- 140 Imai K, Wang L & Carr T D, Modeling Jupiter's Decametric Modulation Lanes, *J Geophys Res (USA)*, 102 (1997) 7127.
- 141 Barbosa D D, Scarf F L, Kurth W S & Gurnett D A, Broadband electrostatic noise and field-aligned currents in Jupiter's middle magnetosphere, *J Geophys Res (USA)*, 86 (1981) 8357.
- 142 Gurnett D A, Frank L A & Lepping R P, Plasma waves in the distant magnetotail, *J Geophys Res (USA)*, 81 (1976) 6059.
- 143 Gurnett D A & Frank L A, A region of intense plasma wave turbulence on auroral field lines, *J Geophys Res (USA)*, 82 (1977) 1031.
- 144 Ashour-Abdalla M & Thorne R M, Towards a unified view of diffuse auroral precipitation, *J Geophys Res (USA)*, 83 (1978) 4755.
- 145 Huba J D, Gladd N T & Papadopoulos K, Lower-hybrid drift wave turbulence in the distant magnetotail, *J Geophys Res (USA)*, 83 (1978) 5217.
- 146 Gray S P & Eastman T E, *J Geophys Res (USA)*, 84 (1979) 7378.
- 147 Matsumoto H, Frank L A, Omura Y, Kojima H, Paterson W R, Tsutsui M, Anderson R R, Horiyama S, Kokubun S & Yamamoto T, Generation mechanism of ESW Based on GEOTAIL Plasma Wave Observation, Plasma Observation and Particle Simulation, *Geophys Res Lett (USA)*, 26 (1999) 421.
- 148 Omura Y, Kojima H, Miki N, Mukai T, Matsumoto H & Anderson R R, Electrostatic Solitary Waves Carried by Diffused Electron Beams Observed by GEOTAIL Spacecraft, *J Geophys Res (USA)*, 104 (1999) 14627.
- 149 Kasahara Y, Hosoda T, Mukai T, Watanabe S, Kimura I, Kojima H & Nitsu R, ELF/ VLF Waves correlated with transversely accelerated ions in the auroral region observed by Akebono, *J Geophys Res (USA)*, 106 (2001) 21123.
- 150 Gurnett D A, Anderson R R, Tsurutani B T, Smith E J, Paschmann G, Haerendel G, Bame S J & Russel C T, Plasma wave turbulence at the magnetopause: Observations from ISEE 1 and 2, *J Geophys Res (USA)*, 84 (1979) 7043.
- 151 Hill T W, Inertial limit on corotation, *J Geophys Res (USA)*, 84 (1979) 6554.
- 152 Dougherty M K, Southwood D J, Balogh A & Smith E J, Field aligned currents in the Jovian magnetosphere during the Ulysses flyby, *Planet Space Sci (UK)*, 41 (1993) 291.
- 153 Das A C, Ip W H, Field-aligned current and particle acceleration in the near-*Io* plasma torus, *Planet Space Sci (UK)*, 48 (2000) 127.
- 154 Kivelson M G, Khurana K K & Walker R J, Sheared magnetic field structure in Jupiter's dusk magnetosphere: Implications for return currents, *J Geophys Res (USA)*, 107 (2002) 1116.
- 155 Cowley S W H & Bunce E J, Origin of the main auroral oval in Jupiter's coupled magnetosphere-ionosphere system, *Planet Space Sci (UK)*, 49 (2001) 1067.
- 156 Hill T W, The Jovian auroral oval, *J Geophys Res (USA)*, 106 (2001) 8101.
- 157 Saur J, Neubauer F M, Strobel D F & Summers M E, Interpretation of Galileo's *Io* plasma and field observations: *Io*, I24, and I27 flybys and close polar passes, *J Geophys Res (USA)*, 107 (2002) 1029.
- 158 Walker R J & Ogino T, A simulation study of currents in the Jovian magnetosphere, *Planet Space Sci (GB)*, 51 (2003) 295.
- 159 Nichols J D & Cowley S W H, Magnetosphere-ionosphere coupling currents in Jupiter's middle magnetosphere : dependence on the effective ionospheric Pedersen conductivity and iogenic plasma mass outflow rate, *Ann Geophys (France)*, 21 (2003) 1419.
- 160 Barbosa D D, Dynamics of field aligned current sources at Earth and Jupiter, Magnetospheric Currents, Edited by T A Potemra, (AGU, Washington DC, USA), 1983, p. 350.
- 161 Oya H & Morioka A, Relations between Turbulent regions of Interplanetary Magnetic Field and Jovian decametric Radio Wave emissions from the Main Source, *Planet Space Sci (UK)*, 29 (1981) 783.
- 162 Goertz C K, *Io*'s interaction with the plasma torus, *J Geophys Res (USA)*, 85 (1980) 2949.
- 163 Bharadwaj A, Gladstone R G & Zarka P, *Io* flux tube footprints in Jupiter's auroral ionosphere, *Adv Space Res (USA)*, 27 (2001) 1915.
- 164 Hospodarsky G B, Christopher I W, Menietti J D, Kurth W S, Gurnett D A, Aerkamp T F, Groene J B & Zarka P, Control of jovian radio emissions by the Galilean moons as observed by Cassini and Galileo, *Planet Radio Emissions*, Vol V, Edited by H O Rucker, M L Kaiser & Y Leblanc. (Austrian Acad Science Press, Austria), 2001, p. 155.
- 165 Delamere P A, Bagenal F, Ergun R E & Su Y J, Momentum transfer between the *Io* plasma wake and Jupiter's ionosphere, *J Geophys Res (USA)*, 108 (2003) 153.
- 166 Hill T W & Vasyliunas V M, Jovian auroral signature of *Io*'s corotational wake, *J Geophys Res (USA)*, 107 (2002) 1462.
- 167 Connerney J E P & Satoh T, The H_3^+ ion: a remote diagnostic of the Jovian magnetosphere, *Phil Trans R Soc (UK)*, 358 (2000) 2471.
- 168 Clarke J T, Ajello J, Ballester G E, Jaffel L B, Connerney J E P, Gerard J G, Gladstone G R, Grodent D, Pryor W, Trauger J & Waite J H, Ultraviolet emissions from the magnetic footprints of *Io*, Ganymede and Europa on Jupiter, *Nature (UK)*, 415 (2002) 997.
- 169 Zarka P, Queinnee J & Crary F, Low-frequency limit of Jovian radio emissions and implications on source locations and *Io* plasma wake, *Planet Space Sci (GB)*, 49 (2001) 1137.
- 170 Gurnett D A, Kurth W S, Roux A, Bolton S J & Kennel C F, Galileo plasma wave observations in the *Io* plasma torus and near *Io*, *Science (USA)*, 274 (1996) 391.
- 171 Bagenal F & Leblanc Y, *Io*'s Alfvén wave pattern and the Jovian decametric arcs, *Astron Astrophys (Germany)*, 197 (1988) 311.
- 172 Erkaev N V, Semenov V S, Shaidurov V A, Langmayr D, Biernat H K & Rucker H O, Investigation of MHD slow shocks propagating along the *Io* flux tube, *J Geomag Aeron (USA)*, 3 (2002) 67.
- 173 Kopp A, Modifications of the electrodynamic interaction between Jupiter and *Io* due to mass loading effects, *J Geophys Res (USA)*, 101 (1996) 24943.
- 174 Linker J A, Kivelson M G & Walker R J, A three dimensional MHD simulation of plasma flow past *Io*, *J Geophys Res (USA)*, 96 (1991) 21037.
- 175 Frank L A, Paterson W R, Ackerson K L, Vasyliunas V M, Coroniti F V & Bolton S J, Plasma observations at *Io* with the Galileo spacecraft, *Science (USA)*, 274 (1996) 394.

- 176 Connerney J E P, Baron R, Satoh T & Owen T, Images of excited H_3^+ at the foot of the *Io* flux tube in Jupiter's atmosphere, *Science (USA)*, 262 (1993) 1035.
- 177 Bagenal F, Alfvén wave propagation in the *Io* plasma torus, *J Geophys Res (USA)*, 88 (1983) 3013.
- 178 Wong H K, Krauss-Varban D & Wu C S, On the role of the energy of suprathermal electrons in the generation of auroral kilometric radiation, *J Geophys Res (USA)*, 94 (1989) 5327.
- 179 Vasyliunas V M, Theoretical models of magnetic field-line merging, *Rev Geophys (USA)*, 13 (1975) 303.
- 180 Arkhipov A V, Search for decametric occultations of *Io* flux tube by Ganymedes, *Astron Astrophys (UK)*, 387 (2002) L25.
- 181 Desch M D & Barrow C H, Direct evidence for solar wind control of Jupiter's hectometer-wavelength radio emission, *J Geophys Res (USA)*, 89 (1984) 6819.
- 182 Barrow C H, Genova F & Desch M D, Solar wind control of Jupiter's decametric radio emission, *Astron Astrophys (USA)*, 165 (1986) 244.
- 183 Genova F, Zarka P & Barrow C H, Voyager and Nancay observations of the Jovian radio emission at different frequencies: solar wind effect and source extent, *Astron Astrophys (USA)*, 182 (1987) 159.
- 184 Zarka P & Genova F, Low frequency jovian emission and solar wind magnetic sector structure, *Nature (UK)*, 306 (1983) 767.
- 185 Broadfoot A L, Belton M J S, Takacs P Z, Sandel B R, Shemansky D E, Holberg J B, Ajello J M, Atreya S K, Donahue T M, Moos H W, Bertaux J L, Blamont J E, Strobel D F, McConnel J C, Dalgarno A, Goody R & McElroy M B, Extreme ultraviolet observations from Voyager 1. encounter with Jupiter, *Science (USA)*, 204 (1979) 979.
- 186 Shemansky D E, Mass-loading and dilution-loss rates of the *Io* plasma torus, *Astrophys J (UK)*, 242 (1980) 1266.
- 187 Bagenal F, The ionization source near *Io* from Galileo wake data, *Geophys Res Lett (USA)*, 24 (1997) 2111.
- 188 Saur J, Neubauer F M, Strobel D F & Summers M E, The ion mass loading rate at *Io*, *Icarus (USA)*, 163 (2003) 456.
- 189 Johnson R E, Energetic Charged-Particle Interactions with Atmospheres and Surfaces (Springer-Verlag, Berlin, Germany), 1990.
- 190 Smyth W H, Energy escape rate of neutrals from *Io* and the implications for local magnetospheric interactions, *J Geophys Res (USA)*, 103 (1998) 26112.
- 191 Linker J A, Khurana K K, Kivelson M G & Walker R J, MHD simulations of *Io*'s interaction with the plasma torus, *J Geophys Res (USA)*, 103 (1998) 19867.
- 192 Combi M R, Kabin K, Gombosi T I, deZeeuw D L & Powell K G, *Io*'s plasma environment during the Galileo flyby: Global three-dimensional MHD modeling with adaptive mesh refinement *J Geophys Res (USA)*, 103 (1998) 71.
- 193 Saur J, Neubauer F M, Strobel D F & Summers M E, Three-dimensional plasma simulation of *Io*'s interaction with the *Io* plasma torus: Asymmetric plasma flow, *J Geophys Res (USA)*, 104 (1999) 25105.
- 194 Saur J, Neubauer F M, Strobel D F & Summers M E, *Io*'s ultraviolet aurora: Remote sensing of *Io*'s interaction, *Geophys Res Lett (USA)*, 27 (2000) 2893.
- 195 Strobel D F, Zhu X & Summers M E, On the vertical thermal structure of *Io*'s atmosphere, *Icarus (USA)*, 111 (1994) 18.